AFOSR-TR. 87-1580

AD-A187 274

Edward L. Ginzton Laboratory
W. W. Hansen Laboratories of Physics
Stanford, California 94305

CRYOGENIC ACOUSTIC MICROSCOPY

Final Technical Report

for the period

April 1, 1985 - March 31, 1987

DTIC
ELECTE
NOV 17 1987
D

Grant No. AFOSR-85-0168

Principal Investigator:
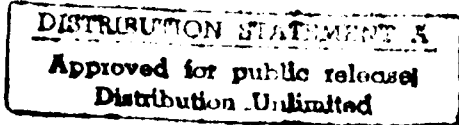
C. F. Quate

Professor of Applied Physics
and Electrical Engineering
Stanford University

G. L. Report No. 4240

August 1987

REPORT DOCUMENTATION PAGE

1a. REPORT SECURITY CLASSIFICATION	1b. RESTRICTIVE MARKINGS
Unclassified	

2a. SECURITY CLASSIFICATION AUTHORITY	3. DISTRIBUTION/AVAILABILITY OF REPORT
2b. DECLASSIFICATION/DOWNGRADING SCHEDULE	Approved for public release; distribution unlimited

4. PERFORMING ORGANIZATION REPORT NUMBER(S)	5. MONITORING ORGANIZATION REPORT NUMBER(S)
G.L. Report No. 4240	AFOSR·TR· 87 - 1 5 8 0

6a. NAME OF PERFORMING ORGANIZATION	6b. OFFICE SYMBOL (If applicable)	7a. NAME OF MONITORING ORGANIZATION
Edward L. Ginzton Laboratory		AFOSR/NE

6c. ADDRESS (City, State and ZIP Code)	7b. ADDRESS (City, State and ZIP Code)
Stanford University Stanford, California 94305	Building 410 Bolling AFB, DC 20332-6448

8a. NAME OF FUNDING/SPONSORING ORGANIZATION	8b. OFFICE SYMBOL (If applicable)	9. PROCUREMENT INSTRUMENT IDENTIFICATION NUMBER
		AFOSR-85-0168

8c. ADDRESS (City, State and ZIP Code)	10. SOURCE OF FUNDING NOS.			
	PROGRAM ELEMENT NO.	PROJECT NO.	TASK NO.	WORK UNIT NO.
		2306/A2		

11. TITLE (Include Security Classification)
Cryogenic Acoustic Microscopy

12. PERSONAL AUTHOR(S)
B. Hadimioglu, C. F. Quate

13a. TYPE OF REPORT	13b. TIME COVERED	14. DATE OF REPORT (Yr., Mo., Day)	15. PAGE COUNT
Final	FROM 4/1/85 TO 3/31/87	1987 August	62

16. SUPPLEMENTARY NOTATION

17. COSATI CODES			18. SUBJECT TERMS (Continue on reverse if necessary and identify by block number)
FIELD	GROUP	SUB. GR	Acoustic microscopy in superfluid helium, Sound waves in superfluid helium, Acoustic transducers

19. ABSTRACT (Continue on reverse if necessary and identify by block number)

This work describes the advancements in the field of acoustic microscopy in superfluid helium at temperatures near 0.1 K. The microscope is presently capable of imaging materials using 300 Å sound waves with 200 Å resolution. Current developments include the search for operation of higher frequencies in order to get better resolution and improvements in the signal-to-noise ratio to get better images.

A new technique has been developed to fabricate high efficiency acoustic transducers at ultra high frequencies. These transducers consist of multilayers of zinc oxide with alternating crystal structure. Multilayer transducers fabricated with the new technique have shown to convert nearly 10% of the electrical input power to acoustic power at frequencies as high as 30 GHz. This is several orders of magnitude better than any of the previous experiments.

/continued on reverse

20. DISTRIBUTION/AVAILABILITY OF ABSTRACT	21. ABSTRACT SECURITY CLASSIFICATION
UNCLASSIFIED/UNLIMITED X SAME AS RPT ☐ DTIC USERS ☐	Unclassified

22a. NAME OF RESPONSIBLE INDIVIDUAL	22b. TELEPHONE NUMBER (Include Area Code)	22c. OFFICE SYMBOL
C. F. Quate	(305) 777 4933	NL

DD FORM 1473, 83 APR   EDITION OF 1 JAN 73 IS OBSOLETE

19. <u>Abstract, continued</u>

Superconducting bolometers have been developed to detect sound waves incoherently. Since these bolometers are also broadband they could detect the harmonics of sound waves generated after nonlinear propagation through superfluid helium.

Sound wave propagation through superfluid helium shows an interesting behavior as liquid helium is dispersive and extremely nonlinear. Experiments have been performed to explore this behavior and how these properties can be used to an advantage. A parametric amplifier system has been tried to potentially improve the signal-to-noise ratio of the microscope by more than 10 dB.

A new mechanical scanner has been developed. The new scanner has the precision required to image samples with better resolution and it features sample changing capabilities while the microscope is cooled at liquid helium temperatures.

TABLE OF CONTENTS

I. INTRODUCTION

This report describes our progress on the development of a cryogenic acoustic microscope capable of imaging materials with very high resolution. We had already operated the microscope at frequencies as high as 8 GHz and examined samples with a resolution of 200 Å.[1] We have concentrated our research on the improvements in the system to image at higher frequencies with even better resolution and with a better signal-to-noise ratio.

As we go to higher frequencies in order to improve the resolution the acoustic transducers appear as crucial elements; they have to operate with high efficiency so as to get a high signal-to-noise ratio of imaging. We have been able to fabricate acoustic transducers that convert nearly 10% of the electrical input power to acoustic power at frequencies as high as 30 GHz. This is several orders of magnitude better than any of the previous experiments. To obtain our results we have used some principles that were proposed as early as 20 years ago but never before demonstrated with experiments at high frequencies because of insufficient technology in the areas of thin-film growth and ultra-high frequency electronics. But today both of these technologies exist and we have been able to combine them to achieve our results.

We have developed superconducting bolometers to detect sound waves incoherently. Since these bolometers are also broadband they could detect the harmonics of the sound waves generated after nonlinear propagation through superfluid helium; hence improving signal-to-noise ratio and giving additional information about samples.

Sound wave propagation through superfluid helium is an interesting phenomenon as liquid helium turns out to be dispersive and extremely

nonlinear. There has been a lot of activity in the recent years to understand the peculiar behavior of sound wave propagation in superfluid helium.[2,3] We have also performed experiments to explore this behavior and how we can take advantage of these properties of liquid helium. We have worked on a parametric amplifier system that exploits dispersive - nonlinear properties of superfluid helium and has the potential to improve the signal-to-noise ratio of the microscope by more than 10 dB.

We have also developed a new mechanical scanner that has the precision required to image samples with better resolution. The scanner also features sample changing capabilities while the microscope is cooled at liquid helium temperatures.

With these developments we are now ready to operate the superfluid helium acoustic microscope at 32 GHz to image samples with 100 Å sound waves.

II. DEVELOPMENT OF HIGH FREQUENCY TRANSDUCERS

Thickness-mode resonant thin-film transducers are commonly used for acoustic wave generation and detection at microwave freqencies. Such structures consist of a thin-film piezoelectric material sandwiched between two metal electrodes deposited on a substrate using standard vacuum deposition techniques. The thickness of the piezoelectric material is near half an acoustic wavelength to get optimum conversion efficiency and bandwidth. An rf-voltage is applied between the electrodes to create an electric field in the piezoelectric layer which generates plane longitudinal sound waves propagating in the substrate. ZnO is generally used as the piezoelectric material because of its high electromechanical coupling constant. It is also suitable for thin-film depositon in the right crystal orientation by vacuum sputtering.[4] Thin-film ZnO transducers are commonly used at microwave frequencies and they are perhaps the most efficient means of sound wave generation and detection at these frequencies.[5,6] Typical two-way conversion loss values of 10-12 dB have been measured at frequencies near 4 GHz with ZnO transducers. These transducers have been fabricated at frequencies as high as 8 GHz and two-way conversion loss values as low as 30 dB were obtained by optimizing the film thicknesses in the transducer structure.[1,6] These transducers, however, have been generally limited to microwave frequencies below 10 GHz. In analogy to electrical antennas, the acoustic radiation from the transducer can be modelled as a radiation resistance for the electrical input port. The acoustic radiation resistance determines the conversion loss of a piezoelectric transducer and it decreases with the square of the frequency[5] causing thin-film ZnO transducers with

reasonable geometries to become very inefficient as the frequency approaches 10 GHz.[6] As an example, the radiation resistance of a 125 μm radius disk transducer is less than 0.1 Ω at a frequency of 8 GHz. Such low resistances are undesirable for two reasons. First, electrically matching the transducer to the 50 Ω characteristic impedance of coaxial cables or nearly 400 Ω impedance of waveguides becomes very difficult. Second, the presence of even small electrical losses in the transducer and the matching network decreases the conversion efficiency of the transducer.[6]

There were also some early efforts to generate sound waves with other piezoelectric materials such as quartz or cadmium sulfide at high microwave or millimeter-wave frequencies. In 1960 Jacobsen used a single crystal quartz placed in a high-Q cavity to generate coherent sound at 24 GHz.[7] This was followed by the work of Thaxter and Tannenwald who performed a similar experiment at 70 GHz.[8] In 1965 Jacobsen and Ilukor extended the frequency of coherent sound wave generation to 114 GHz.[9] They used single crystal quartz and thin-film CdS as piezoelectric materials. Although these experiments proved that coherent sound wave generation is possible at these high frequencies, the high value of the conversion loss was a major problem. The conversion loss values were estimated to be greater than 80 dB even at 24 GHz. The high-Q cavity used also limited the frequency of operation to a small range. Because of these problems these experiments did not attract much interest. All three of these experiments use surface excitation for the generation and detection of the sound,[10] similar in principle to the method in the thin-film resonant devices described above. The reason behind the low conversion loss again could be found in the low radiation resistance for the transducer structure. Therefore, it is desirable to use a method to increase the radiation resistance of acoustic transducers to improve the impedance

matching and to decrease the conversion loss. One method to achieve this is to use a periodic multilayer structure.

II.A. MULTI-LAYER ACOUSTIC TRANSDUCERS

The history of generating coherent sound with periodic multi-layers goes back some twenty years. In 1965 Shaw[11] and de Klerk et al.[12] realized that the transducer efficiency could be improved with multi-layers of piezoelectric materials forming a periodic structure. Such structures consist of alternating layers of piezoelectrically active and inactive (or less active) materials with a period equal to the acoustic wavelength. The radiation resistance increases as the square of the number of active layers in such a structure.[12,13] Hence, one would like to use as many layers as possible. De Klerk et al.[12] used multilayer CdS-SiO transducers to show the improvement in the efficiency near 1 GHz. Conversion loss improvements of 6 and 9.5 dB compared to single-layer were reported at 1 GHz for 3 and 5 layer CdS-SiO structures, respectively.[12] In 1973 Yang et al.[14] pointed out that the advent of superlattices made it feasible to use periodic layers to generate coherent phonons at frequencies from millimeter-wave to infrared. This was followed in 1982 by the work of Wong et al.[15] where they discussed superlattices made with materials with strong piezoelectric coupling coefficients. In 1982 other suggestions for generating coherent phonons appeared in the work of Ruden and Döhler[16] and Quinn et al.[17] They described a superlattice of a nonpiezoelectric semiconductor with layers of alternating charge, the so-called n-i-p-i structures. Dransfeld has elaborated on these systems in his presentation at the symposium on Rayleigh waves.[18]

Here we first describe a new technique to fabricate very efficient multilayer acoustic transducers at millimeter-wave frequencies, using ZnO with alternate crystal structure.[19]

II. A.1. MULTILAYER TRANSDUCER FABRICATION

ZnO is very desirable to use in multilayer transducers because of its high piezoelectric coupling constant. Therefore, it is possible to obtain a reasonably high radiation resistance with a relatively small number of layers. One constraint on the fabrication of multilayer ZnO transducers is that the entire deposition should be done in one single pump-down. This is required for ease of fabrication and prevention of contamination of the transducer by exposure to air, thus preventing any adhesion problems in the multilayer structure. This requirement becomes especially important in a multilayer transducer at millimeter-wave frequencies where several layers are required to get a significant improvement in the conversion loss. Currently we deposit ZnO by dc-magnetron sputtering from a zinc target in a 80%-20% oxygen-argon atmosphere in a vacuum system dedicated to ZnO growth and it is undesirable to introduce materials other than the ones mentioned above in the station, so as to avoid contaminating the sputtering system.

It is possible to fabricate a multilayer structure that satisfies our deposition requirements simply by alternating the orientation of the ZnO film. The optimal coupling between electrical and longitudinal acoustic fields is obtained when the c-axis of ZnO is oriented parallel to the applied electric field. As the c-axis is rotated from the normal direction, the acoustic coupling becomes weaker. The longitudinal coupling coefficient becomes zero when the angle between the c-axis and the electric field is 40°. It has been shown that thin-films of ZnO can be

grown with the c-axis at a finite angle to the normal to the substrate by tilting the substrates and positioning them near the edge of the plasma in the sputtering station.[20] Since the ZnO grows with the c-axis normal to the substrate when it is positioned above the center of the target, one can grow a multi-layer transducer simply by moving the samples back and forth between these positions during deposition. A conceptual diagram of multilayer ZnO transducers is shown in Figure 1.

Figure 2 shows a diagram of the set-up for the deposition of multilayer transducers. The substrate holder in the basic ZnO station is replaced by a system that can position the substrate at 3 different locations. At position I, the pieces are parallel to the zinc target and centered opposite the target. This positioning yields "normal" ZnO with high piezoelectric coupling coefficient. At positions II and III the pieces are moved a distance d from the center of the target and angled approximately 40° with respect to the target normal. At these angled positions we expect to grow ZnO with lower piezoelectric coupling. The holder is moved between these positions in the order of I-II-I-III-I-II... to deposit a multilayer transducer. The reason for using both of the positions II and III is to equalize any thickness variations on the substrates in the direction parallel to the movement of the substrate holder. This is especially important when a structure with a large number of layers is fabricated. The substrate holder has 6 holes to place the samples numbered from 1 to 6 as shown in Figure 2(b). It should be mentioned that the holder does not have circular symmetry as the holes have different separations to the center of the station. As a result some differences may be expected between samples mounted near the edge and the middle of the holder.

MULTI-LAYER TRANSDUCERS

GOLD BOND WIRE

2000 Å GOLD TOP-ELECTRODE

1000 Å GOLD COUNTER-ELECTRODE

SAPPHIRE SUBSTRATE

NORMAL ZnO 4000 Å THICK ($\lambda/2$ @ 8 GHz)

TILTED ZnO 4000 Å THICK ($\lambda/2$ @ 8 GHz)

FIG. 1-- Conceptual diagram of multi-layer ZnO transducers.

(a)

III — **II**

I

2"

d — d

Zn TARGET

HOLES FOR
SUBSTRATES

(b)

#1
2
3
4
5
6
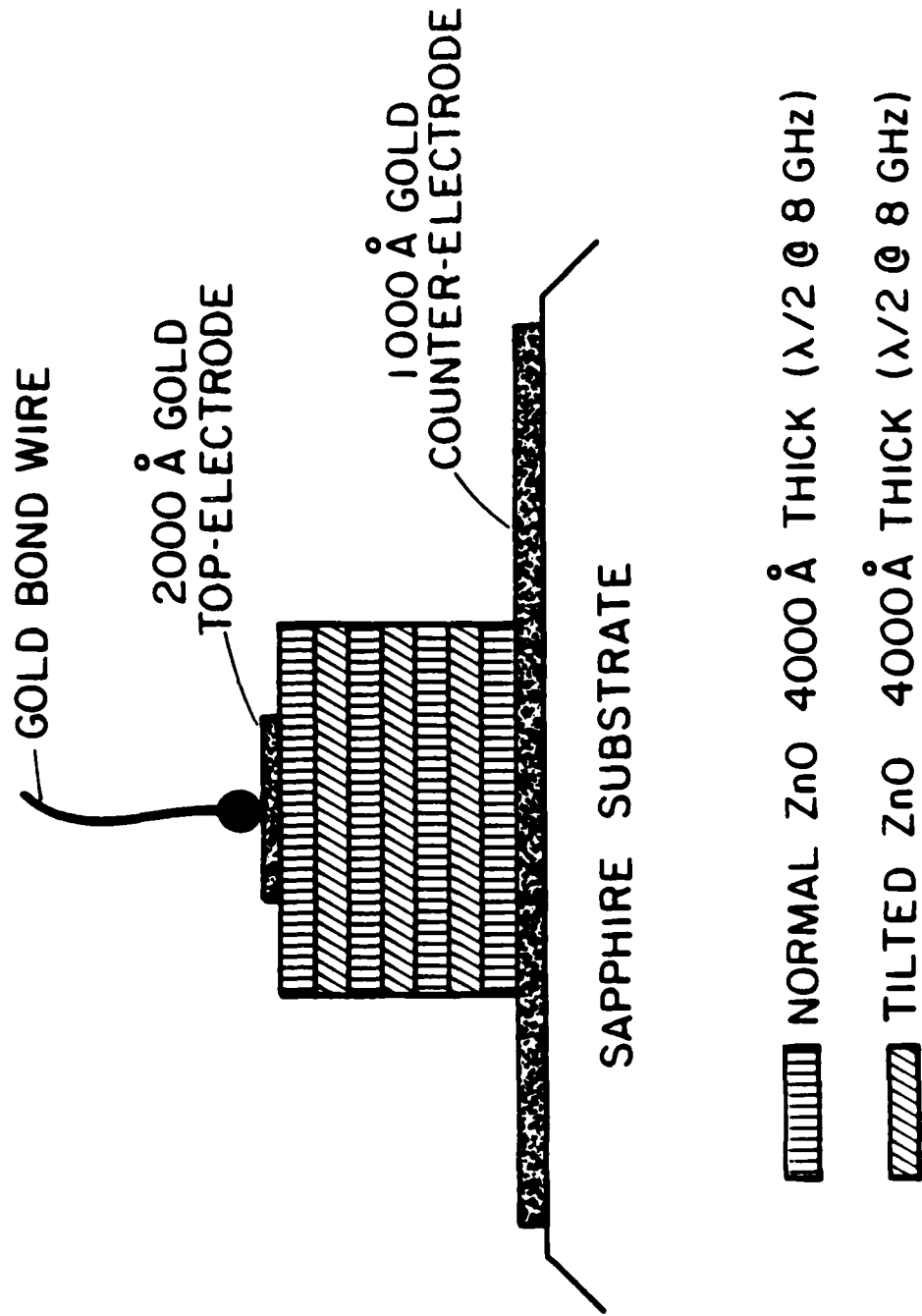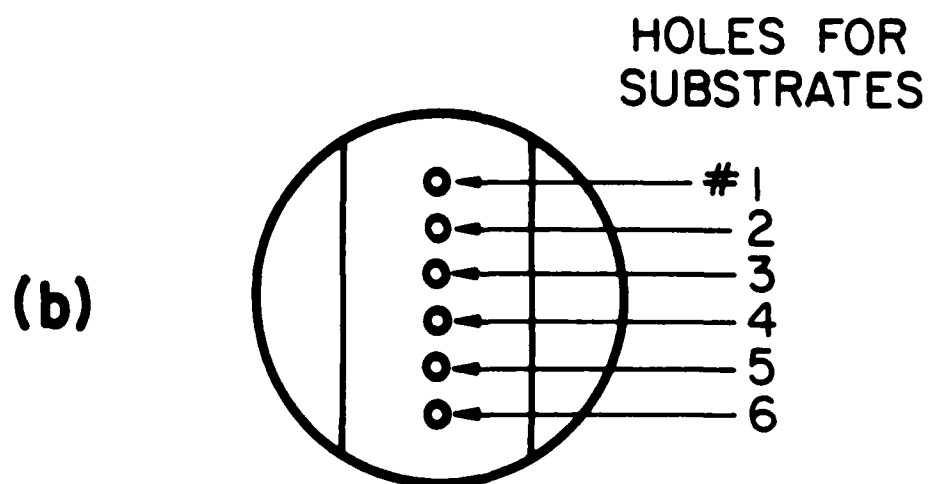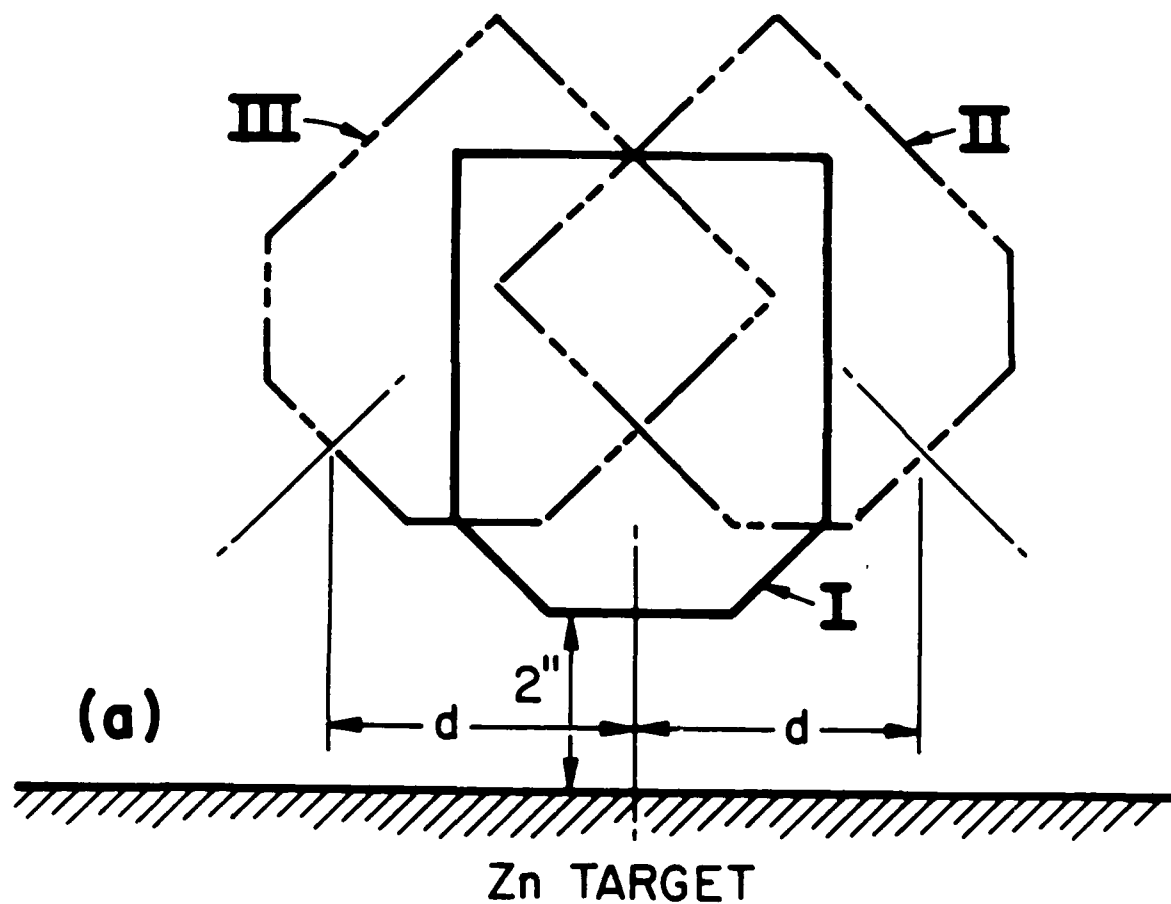
FIG. 2-- (a) Cross-sectional view of the multi-layer transducer fabrication
procedure. (b) Bottom view of the substrate holder.

II.A.2. RESULTS AT LOW FREQUENCIES

We first tested the idea of ZnO multi-layers by depositing single-layer thin films of ZnO at positions I and II and comparing the acoustic properties of these layers (Positions II and III are symmetrical for the deposition of single-films, so it is not necessary to compare the films deposited at both angled positions to the transducers fabricated at the center of the plasma). The single-layer transducers were designed for operation near 8 GHz and had the following physical characteristics:

ZnO thickness	4000 Å (half-wave at 8 GHz)
Transducer radius	125 μm
Counter-electrode	2000 Å Ti/Au
Top-electrode	2000 Å Cr/Au
Substrate	Sapphire

Figure 3(a) and (b) show the room temperature two-way conversion losses measured for two transducers deposited at positions I and II, respectively. The distance d as defined in Figure 2 for the transducer in Fig. 3(b) is 1.5 inches. We have also analyzed the transducer structure using the Mason model for the transducer[5] to determine the piezoelectric coupling constant that gives the best match between the theoretical and experimental responses for each transducer. We have found that the coupling constants for cases (a) and (b) are 0.25 and 0.16, respectively. The coupling constant measured for case (a) is very close to that for bulk ZnO which proves that the "normal" ZnO film has nearly single crystal characteristics with the c-axis oriented perpendicular to the substrate. The mechanical coupling measured for the transducer deposited at position II is approximately 50% lower. Hence a transducer fabricated by alternatively stacking up these layers should offer significant improvement in the conversion loss. It should be noted that no significant

NORMAL ZnO vs ANGLED ZnO
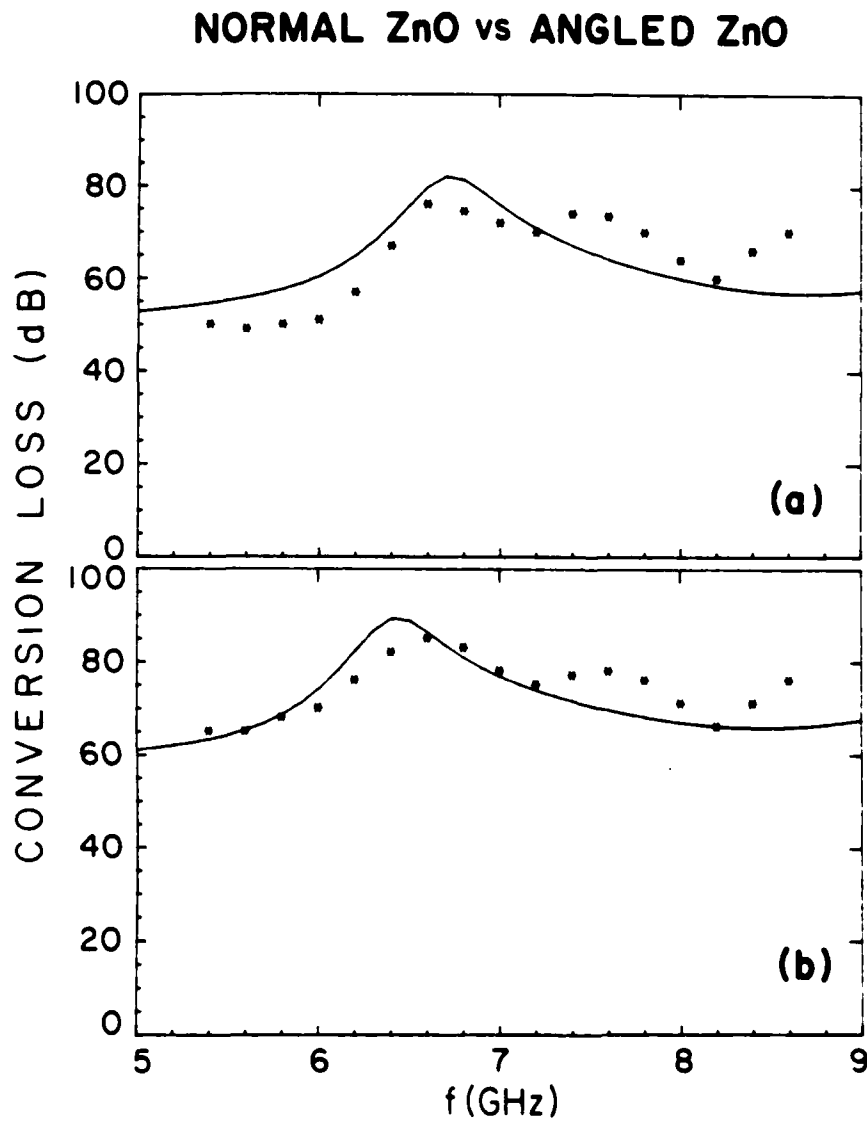
FIG. 3-- (a) and (b) Measured untuned conversion loss (dots) for transducers deposited at positions I and II, respectively. The solid lines were calculated using Mason's model for the transducers.

shear wave generation was observed for the transducer in case (b), which indicates that the layer grown at position II has more of an amorphous character rather than simple c-axis tilting reported in Reference 20.

We have fabricated multilayer transducers by moving the substrate between the positions I, II and III as described above. Figure 4(a) shows the two-way untuned and tuned conversion losses measured for one of the multilayer transducers. The transducer was designed for operation at 8 GHz and was composed of 7 normal and 6 angled half-wave layers of ZnO. The remaining transducer parameters were the same as for the single-layer transducers except for the counter-electrode thickness which was 1000 Å. It can be seen that the insertion loss of the multilayer transducer has approximately 20 dB improvement over the single-layer case plotted in Figure 3(a) near the center frequency of 8 GHz. The untuned conversion loss was also measured at a temperature of 77 K as plotted in Figure 4(b). The conversion loss shows an improvement of over 10 dB between 300 K and 77 K at the center frequency near 8 GHz. We also tried fixed tuning of the transducer and then cooling to liquid helium temperatures. Figure 5 compares the measured two-way tuned conversion loss of a multilayer transducer to that of a single-layer transducer both operating at 4 K. Both transducers were tuned at room temperature near 8.4 GHz to take the temperature variations in the microwave matching network into account.[1] The two-way tuned conversion-loss at the center frequency for the multilayer transducer is only 12 dB which is 18 dB better than the single-layer case. The bandwidth of the transducer is approximately 200 MHz, approximately the same as the single-layer transducer.

It should be noted that the multilayer transducers mounted in holes 1 and 6 in the substrate holder during ZnO deposition always showed the

5695-'A

# MULTI-LAYER TRANSDUCER AT 8 GHz

• UNTUNED LOSS
• TUNED LOSS
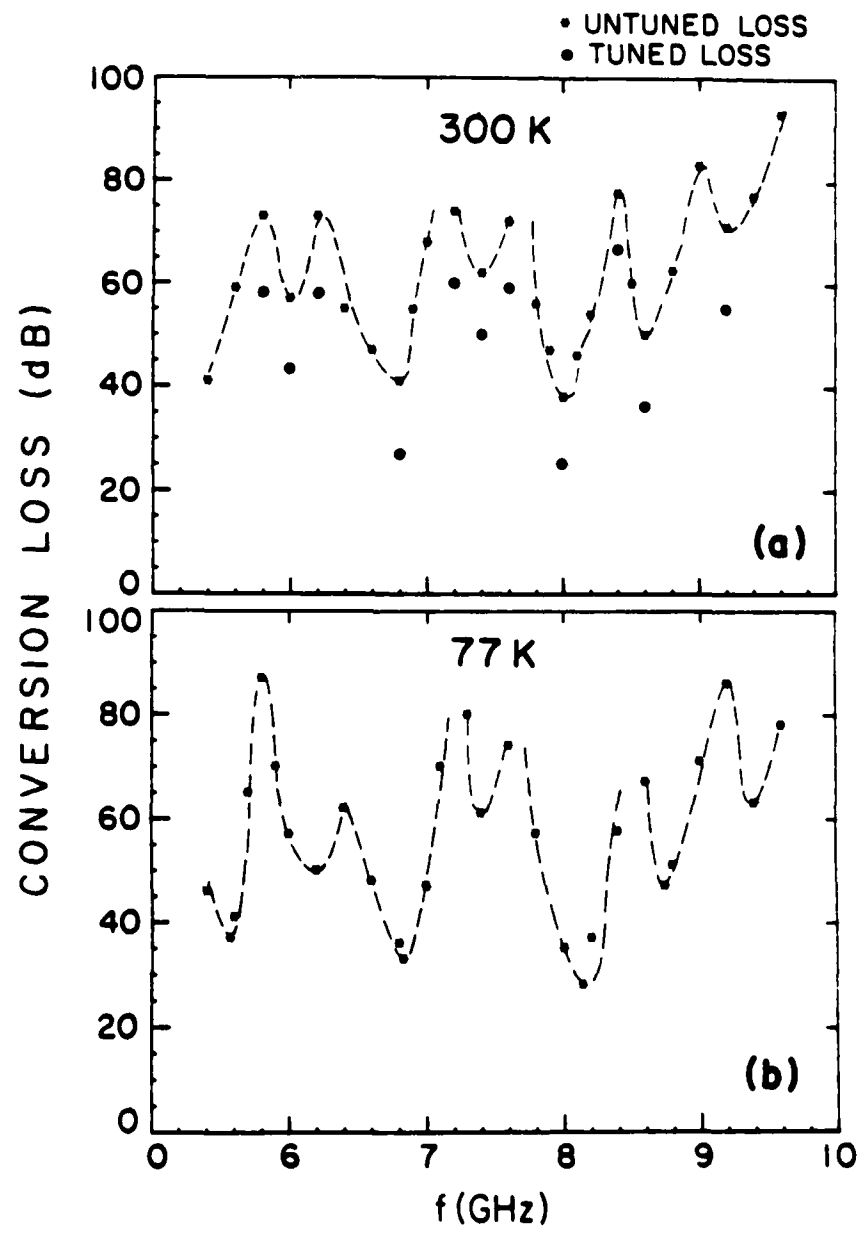
FIG. 4-- Measured two-way conversion loss for a multi-layer
transducer designed for 8 GHz operation. (a) Temperature
300 K, (b) Temperature 77 K.
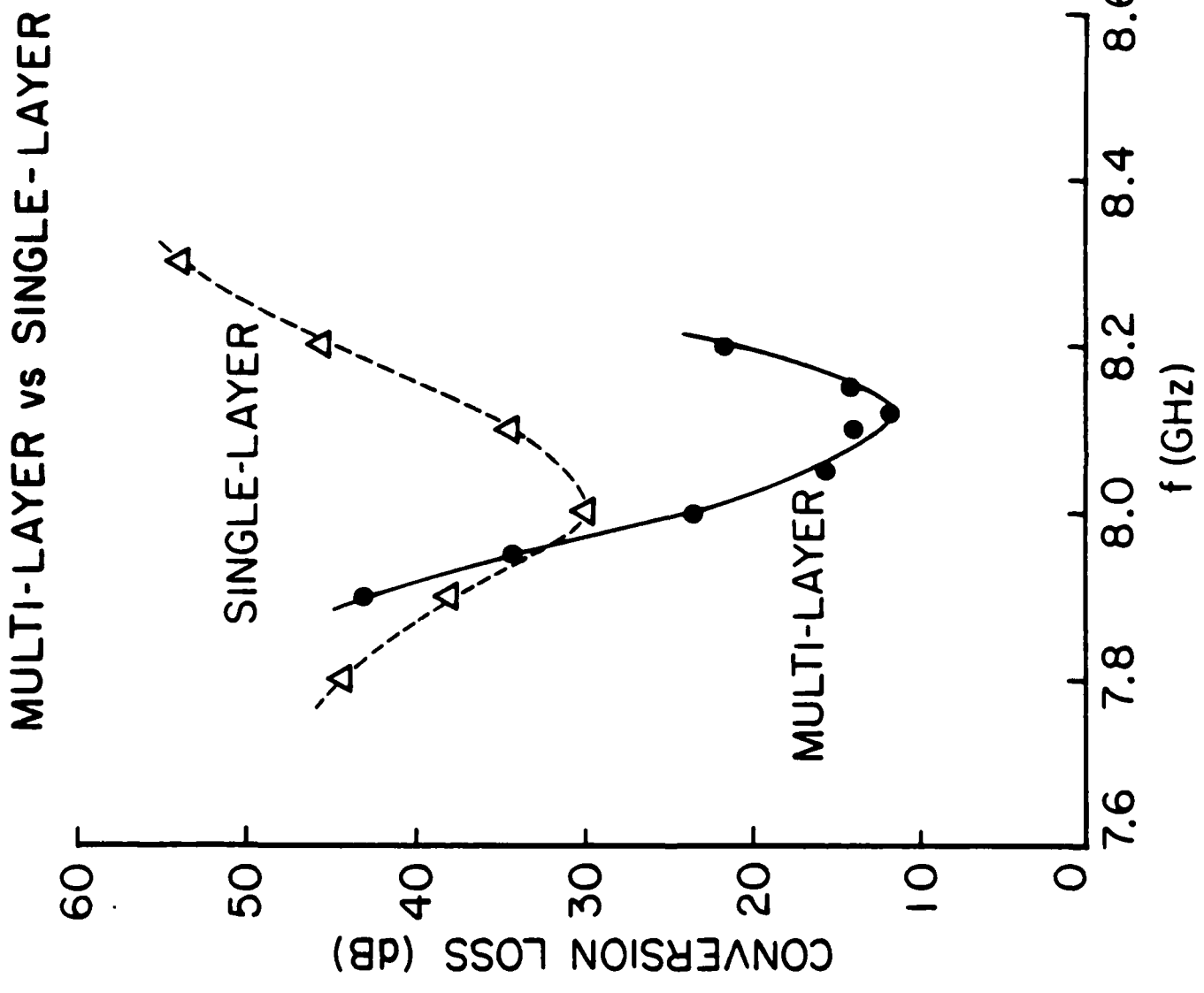
FIG. 5-- Comparison of two-way tuned conversion loss for single- and multi-layer transducers. Temperature is 4 K.

best response. The transducers fabricated in holes 3 and 4 had nearly 20 dB higher conversion loss. This behavior can be explained by the observation that the angled films deposited in holes 1 and 6 had lower piezoelectric constants compared to the ones in 3 and 4. Greater modulation of the piezoelectric constant for the multilayer transducers fabricated in holes 1 and 6 results in the improvement in the conversion loss.

We have also fabricated multilayer structures for operation at 12 GHz. Figure 6 shows the tuned and untuned conversion loss of a multilayer transducer measured at 300 K and 77 K. The transducer is again composed of 13 layers of normal and tilted ZnO layers. Each layer is 2700 Å thick. It can be seen that the minimum low-temperature tuned conversion loss is approximately 22 dB around 12 GHz. This is nearly 10 dB better than the value measured for single-film tranducers operating under similar conditions. Figure 6 also shows stronger acoustic resonances near 8 and 10 GHz. The reason for this behavior is still unknown and is being investigated using a theoretical model for the transducer.

II.A.3. MULTILAYER TRANSDUCERS AT MILLIMETER-WAVE FREQUENCIES

We continued on the use of this technique to generate acoustic waves at millimeter-wave frequencies in the Ka-band (26.5-40 GHz). Extrapolating the results of the 12 GHz experiment, we designed and fabricated multilayer ZnO transducers for operation around a center frequency of 32 GHz. The physical characteristics of the transducer structure are listed below.

ZnO thickness (each layer)	950 Å
Total number of ZnO layers	15
Transducer radius	20 μm

MULTI-LAYER TRANSDUCER AT 12 GHz
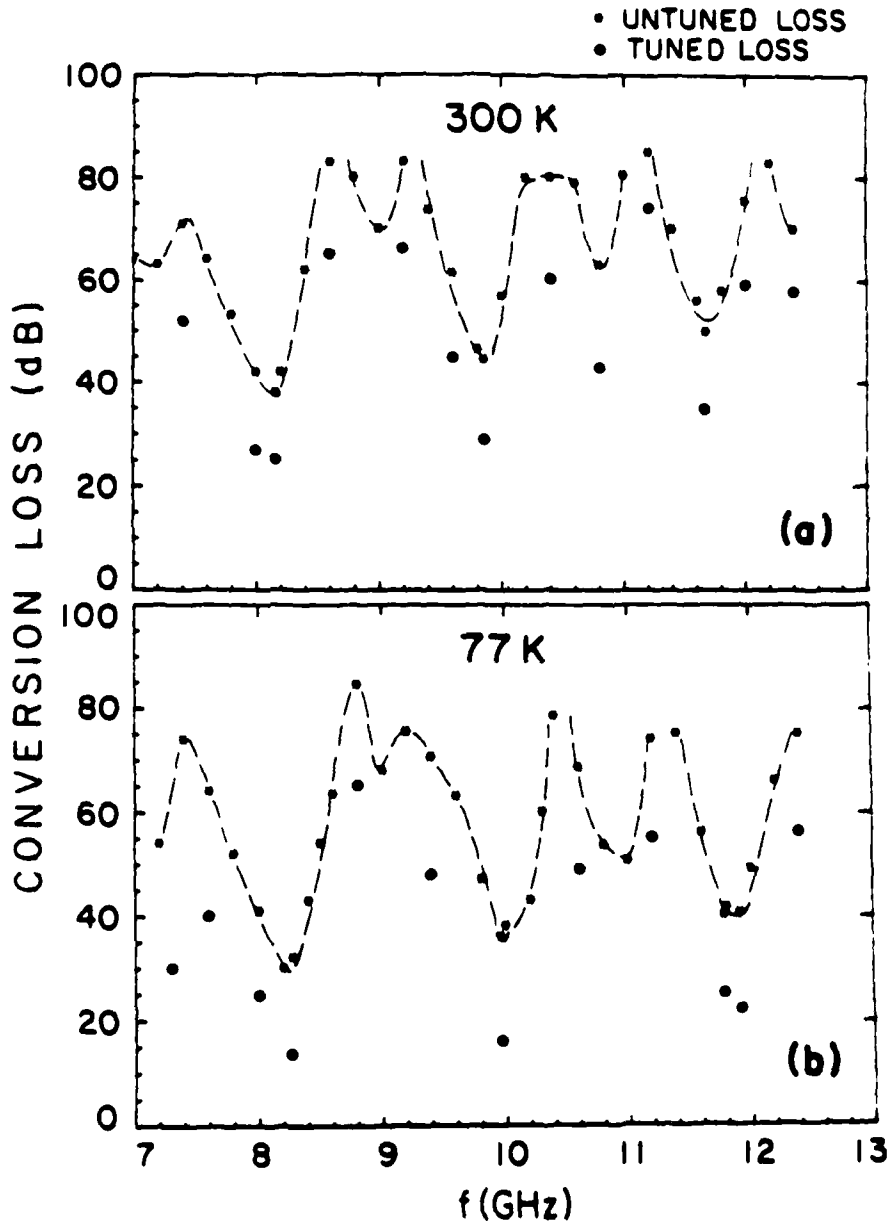
FIG. 6-- (a) 300 K and (b) 77 K measured conversion loss for a
multi-layer transducer designed for 12 GHz.

- 16 -

Counter-electrode	1000 Å Ti/Au
Top-electrode	1500 Å Cr/Au
Substrate	Sapphire
Substrate thickness	2.6 mm

The electrical coupling to the transducer was achieved by using a 50 μm diameter gold wire thermo-compression bonded to the top-electrode of the transducer. Since the transducer was too small for direct bonding of the wire, an offset top-electrode technique[21] was used. The other end of the wire was connected to a microstrip line with a characteristic impedance of 50 Ω using indium solder. The length of the wire was kept very short (less than 0.5 mm) to minimize the series reactance. An SMA connector at the other end of the microstrip line was used to bring the electrical signals in and out of the transducer. The counter-electrode of the transducer was pressure contacted to the ground plane of the microstrip line.

The acoustic attenuation in the 2.6 mm long sapphire substrate is larger than 50 dB at room temperature. To reduce the attenuation to reasonable levels, the measurements were taken after cooling down the substrate in liquid nitrogen at a temperature of 77 K. Figure 7 shows the measured two-way untuned conversion loss values as a function of frequency for the best transducer. It can be seen that the minimum value of the conversion loss is 30 dB at a frequency of 28.6 GHz.

It must be noted that the results plotted in Figure 7 contain some losses in the sapphire substrate. These losses are mainly due to diffraction and acoustic attenuation in the sapphire rod. The diffraction in sapphire was calculated[22] for propagation along the c-axis of sapphire as a function of propagation distance in Fresnel lengths. For the 20 μm radius transducer at 28.6 GHz we have a round trip propagation distance of
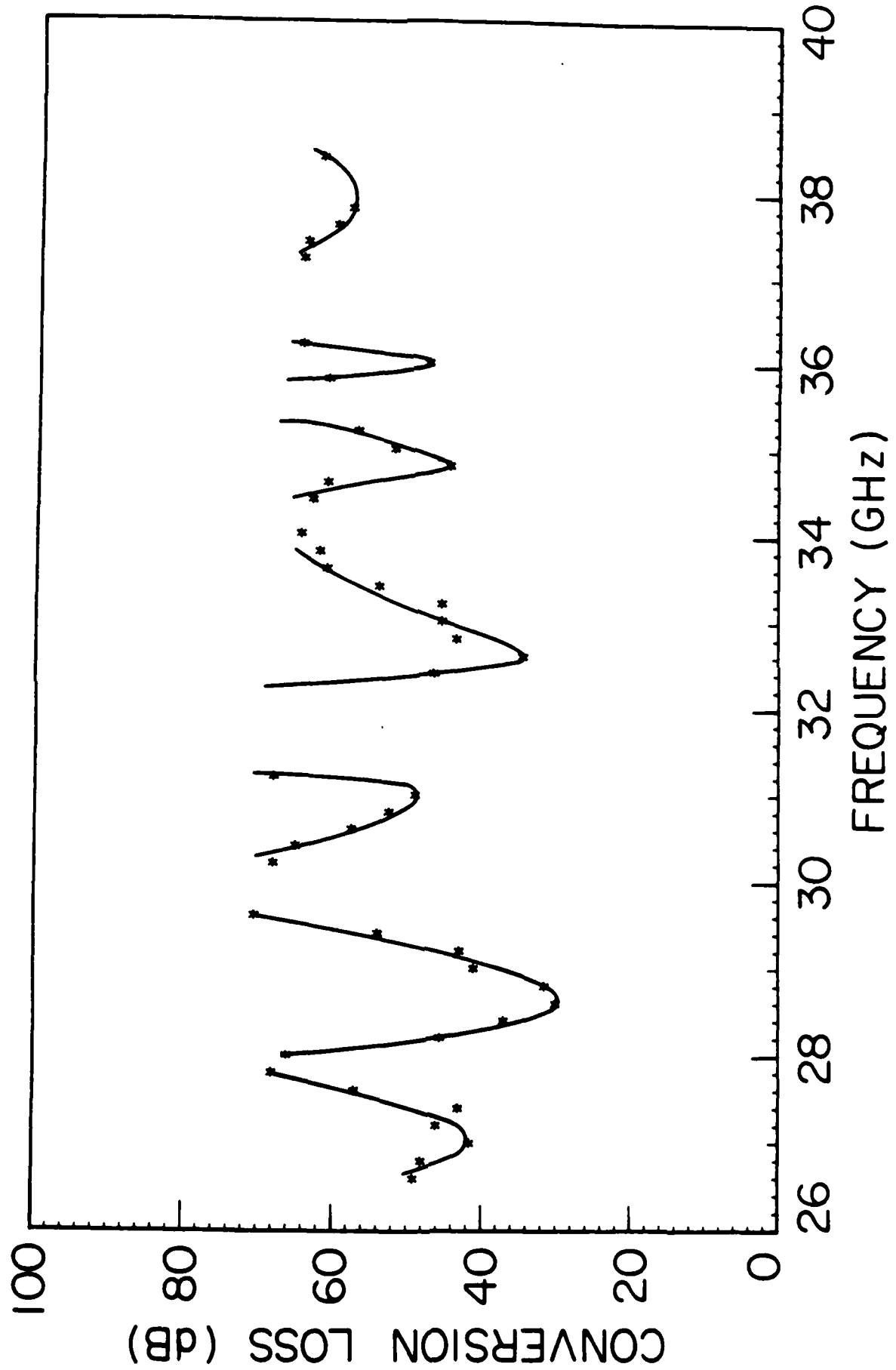
FIG. 7— Two-way untuned conversion loss as a function of frequency for a Ka-band transducer at 77 K. The solid lines are a smooth fit to the data.

5.2 Fresnel lengths resulting in a loss of 3.2 dB. Assuming a linear frequency dependence of attenuation and extrapolating the sound attenuation from 3.0 GHz,[23] we find approximately 2 dB of acoustic loss for the 5.2 mm path in the sapphire. Additional losses in the sapphire can occur because of the transducer's coherent sound generation and detection properties. Since the sound wavelength in sapphire is only 4000 Å, the surfaces of the sapphire substrate should be extremely parallel and flat to minimize these losses. The presence of these losses is easily determined by looking at the pattern of multiple reflections in the substrate. An exponentially decaying echo-pattern indicates a good substrate in terms of parallelism and flatness. Figure 8 shows the multiple reflections obtained with the transducer in Figure 7. The sum of the calculated diffraction and acoustic losses are in good agreement with the difference between successive reflections of approximately 6 dB indicating good substrate parallelism and flatness. An upper limit on the conversion loss in the transducer can be found by subtracting the loss due to diffraction from the data in Figure 7. This calculation gives a two-way conversion loss of 27 dB at 28.6 GHz.

It should be noted here that the measurements in the experiment above were taken with the transducer connected to the microstrip line via a gold wire. The input resistance of the transducer was estimated to be around 1 Ω resulting in a large electrical impedance mismatch between the transducer and the transmission line. Thus most of the incoming electrical energy was reflected back without being delivered into the transducer (like driving the tranducer with a heavily overcoupled cavity). It should therefore be possible to improve the conversion loss of the transducer by using an electrical impedance matching network (or using a critically coupled cavity) to drive the transducer. We tried a simple

ACOUSTIC REFLECTIONS
IN SAPPHIRE

FREQUENCY = 28.6 GHz
TEMPERATURE = 77 K
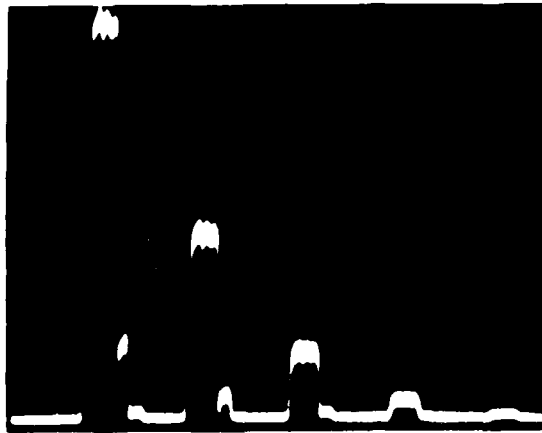
FIG. 8-- Echo pattern of 28.6 GHz sound waves
in sapphire at 77 K.

tuning technique by using a parallel stub on the microstrip line. This resulted in an improvement of 7 dB at Ka-band giving a two-way conversion loss of 20 dB at 28.6 GHz. This result is several times better than any of the experiments previously done at such high frequencies. A conversion loss of 20 dB should be also small enough for acoustic microscopy in superfluid helium near 30 GHz with an acceptable signal-to-noise ratio.

III. BOLOMETERS FOR INCOHERENT PHONON DETECTION

The acoustic transducers previously mentioned detect sound waves coherently, that is, they respond to the phase and amplitude of the incident sound radiation. Another method of sound detection is to use a bolometer, which measures the incident *energy* of the sound without regard for coherence. Thus the bolometer can be referred to as an incoherent phonon detector - it counts the number of incident phonons.

Bolometers are typically made with materials where the resistance varies as a function of temperature. The sensitivity of the bolometer depends on the strength of temperature dependence. For this reason, superconductors are often used for bolometers due to their extreme temperature sensitivity at the critical temperature that defines the superconducting transition. The operation of the superconducting bolometer is as follows. The superconductor is biased (either with temperature, current, or magnetic field) so that its resistance is just on the low side of the resistive transition. If an acoustic pulse is incident on the superconductor it will warm slightly, causing the resistance to climb as the superconductor becomes more "normal." The resistance change can be measured by passing a constant current through the superconductor and measuring the change in voltage.

Bolometers could have three important uses for our research. First, because they are not sensitive to the phase of the incoming phonons, the imperfections in the substrate crystal such as non-parallelism and flatness of the surfaces will not degrade the signal amplitude. We have seen previously that with piezoelectric transducers such imperfections cause problems with the detection scheme, especially at high frequencies,

making it difficult to perform some experiments such as the measurement of the sound attenuation in the substrate.

Second, the bolometers have some potential to improve the signal-to-noise ratio of detecting phonons relative to acoustic transducers. At the present time, transducers are a much more sensitive detector of coherent sound radiation than bolometers for frequencies of 8 GHz and under. As we go to higher frequencies, however, transducers become less efficient. Unlike transducers, bolometers generally become more sensitive for detecting high frequency phonons. This is because high frequency phonons, as they go through the bolometer material, have a higher scattering rate, giving up more energy to the material and heating it to higher temperatures.

The third important use for bolometers is they are inherently broadband because they are only energy sensitive. The piezoelectric transducers we have described are generally narrowband. We know that the sound propagating in superfluid helium tends to generate harmonics, but these are undetectable with our transducers because of bandwidth limitations. Incoherent bolometers should be able to detect the harmonics of the transmitted sound waves, improving the signal-to-noise ratio of the microscope and also helping us understand the nonlinear properties of low temperature liquid helium.

To begin our work on bolometers we first visited V. Narayanamurti's laboratory at AT&T Bell Laboratories to learn their state-of-the-art bolometer-receiver methodology. Since then we have fabricated and demonstrated our own bolometers. An example of an experiment is shown in Fig. 9(a). The bolometer is a thin-film aluminum, electron-beam deposited at room temperature with 5×10^{-6} torr of oxygen background pressure. The oxygen causes defects in the aluminum film and raises the
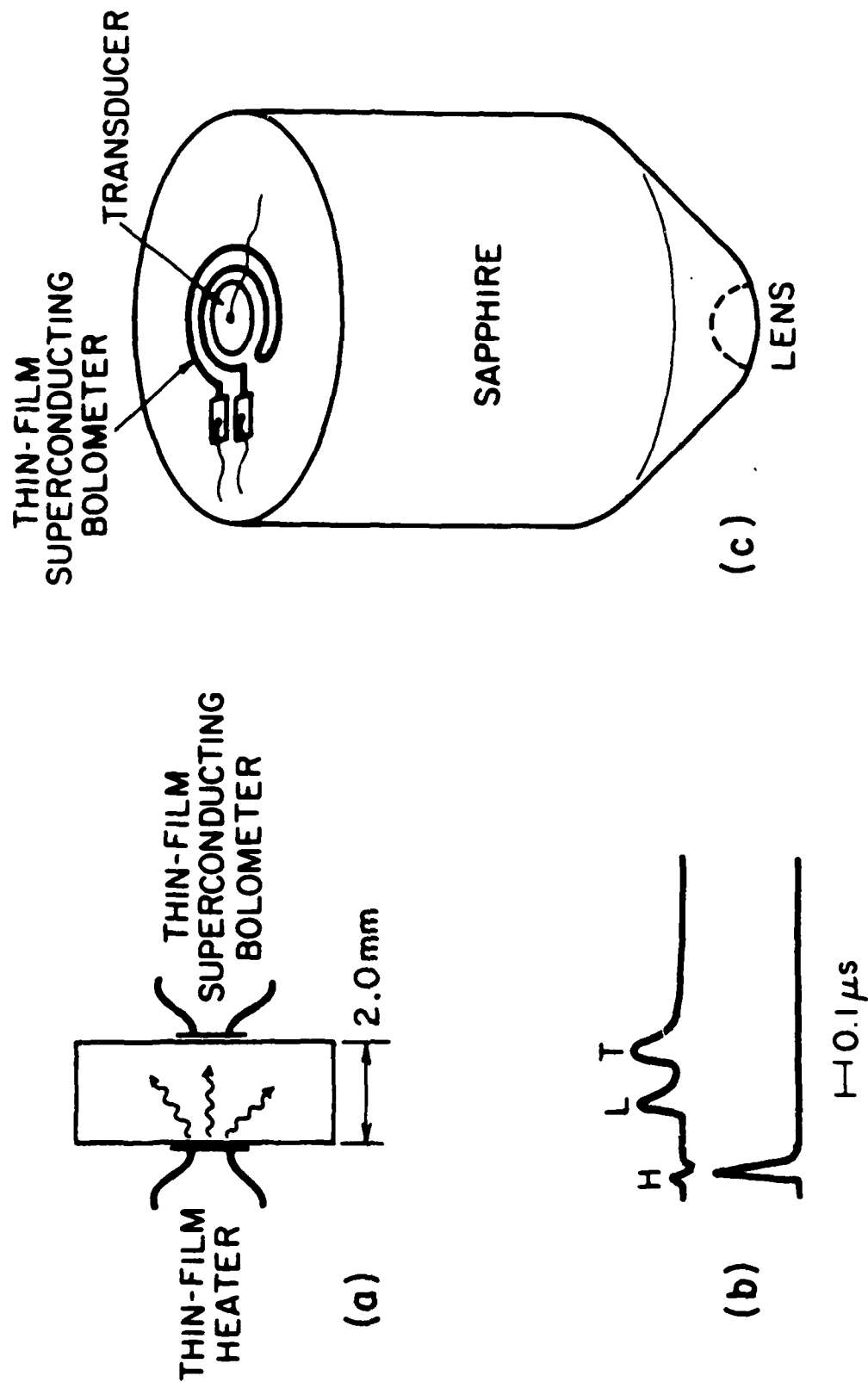
FIG. 9-- (a) The experiment for detection of thermal phonons from a thin-film heater using a superconducting bolometer. (b) A trace showing the detected longitudinal and transverse phonons. (c) Diagram of the bolometer-acoustic transducer to be used on the acoustic lens.

critical temperature so that the bolometer can be tested in a simple pumped helium-4 bath (T = 1.3 K). (The superconducting critical temperature for pure aluminum is about 1 K and goes up to 1.4 -1.7 K with oxygen.) The aluminum bolometer in Fig. 9(a) has been deposited on a sapphire slab. On the opposite face of the slab, a thin-film of chrome (500 Å thick) has been deposited. When a current pulse is passed through the chrome, a pulse of thermal phonons is launched into the sapphire and can be detected by the bolometer as shown in the Figure. Two thermal phonon pulses are actually detected because the longitudinal and transverse phonons separate in time due to their differing sound speeds. The data in Fig. 9(b) demostrate the fast time response (< 100 ns) which is required to separate the multiple echoes in the substrate. In addition to detecting thermal phonons, we have also fabricated a bolometer next to an acoustic transducer and measured coherent sound radiation at 4 GHz. Fig. 9(c)shows how the bolometers can be employed in the fabrication of an acoustic lens to launch and detect focused sound waves in superfluid helium. The bolometer is in a ring shape surrounding the acoustic transducer and it detects the phonons falling outside the transducer. Therefore, it is possible to detect phonons both coherent, narrowband (using the tranducer) and incoherent, broadband (using the bolometer) simultaneously with this scheme.

IV. SOUND WAVE PROPAGATION IN PRESSURIZED SUPERFLUID HELIUM

The signal-to-noise ratio of the acoustic microscope can be increased very simply by applying pressure to the superfluid helium which acts as the coupling fluid between the lens and the sample. There is an effective attenuation of sound due to three-phonon processes in the liquid helium. This process, however is very sensitive to the sound dispersion in the helium, which is, in turn a function of pressure.

Figure 10 depicts a three-phonon scattering event in which two phonons collide and form a third phonon. (The reverse process also occurs.) The collision conserves energy and momentum. The phonon energy is $h\omega/2\pi$, and so conservation of energy requires $\omega_1 + \omega_2 = \omega_3$. The phonon momentum is $hk/2\pi$, and so conservation of momentum requires $k_1 + k_2 = k_3$.

If there were no dispersion, i.e., $\omega = c_0 k$ for all frequencies, and c_0 is a constant speed, then the two conservation equations require that the phonons be collinear - all momenta in the same direction. If the dispersion is upward as shown in Figure 10, then the sound speed c is increasing with frequency. In this case, we see from the Figure that the higher energy phonon ω_3 will have less momentum than the no dispersion case. Then the two input phonons, ω_1 and ω_2 must intersect at a finite angle so that some of their momentum will be cancelled, and the momentum will then be conserved. We thus see that the drawing in Figure 10 is representative for the upward dispersion case. If the dispersion is downward, the higher energy phonon ω_3 has too much momentum, which cannot be obtained from ω_1 and ω_2. Hence, if the dispersion is downward,

- 26-

THREE PHONON SCATTERING
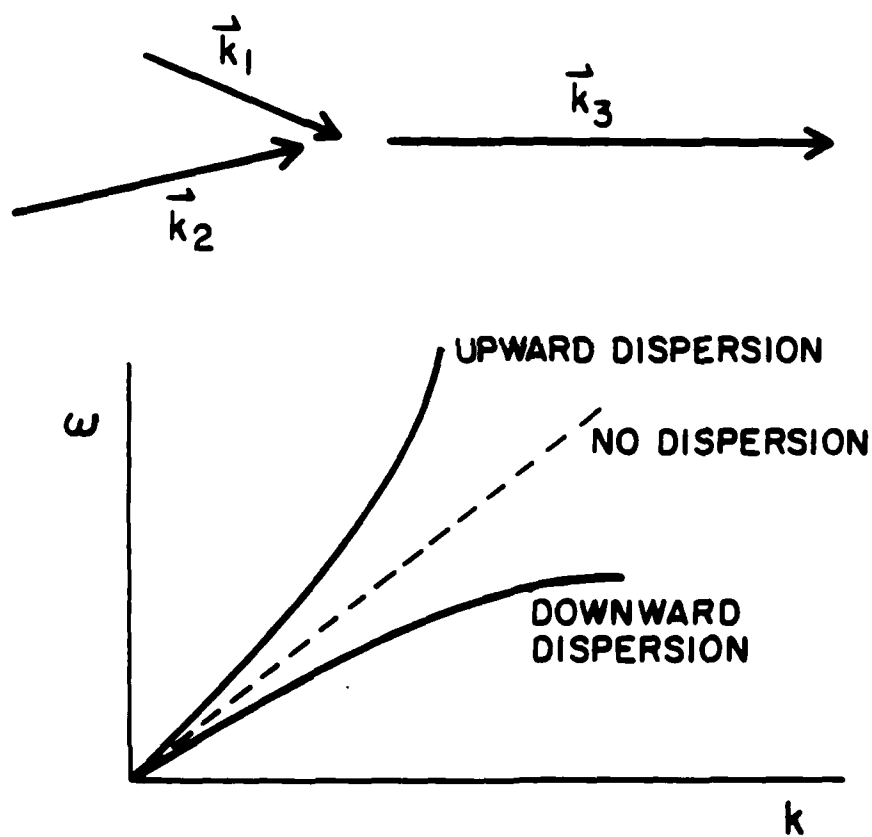
FIG. 10-- Diagram showing the scattering of two phonons to form a
third one for various dispersion cases.

the three-phonon process cannot conserve energy and momentum and thus becomes quite unlikely.

We are fortunate that in superfluid helium the dispersion is adjustable. At low pressures, the dispersion is upward, and so three-phonon collisions occur at a finite angle. As pressure is applied, the dispersion becomes more linear and above 20 bar, the dispersion is downward. Hence, above 20 bar the helium should be more transparent for sound, and the signal-to-noise should increase.

There is an additional change in helium when pressure is applied : several liquid parameters change such as the density, sound speed, and nonlinearity. All of these parameters shift the scattering amplitudes of the three-phonon processes down as the pressure is increased, helping the signal-to-noise ratio of the acoustic microscope.

To test the pressure dependence of the signal-to-noise ratio we placed an acoustic lens and a reflector in a pressure cell (Figure 11). The cell has been described previously.[2] The cell allows the lens-sample spacing to be adjusted, and, of course,allows the application of pressure to liquid helium up to 25 atmospheres at which point liquid helium freezes. In the experiment we measured the intensity of sound pulses which bounce off the reflector (flat sapphire) and returns to the acoustic lens. The received signal is plotted in Figure 12 as a function of pressure in the cell for two frequencies with two different acoustic lenses. It can be seen that although the shape of the curve is considerably different between 7 and 8 GHz, there is a 20 dB increase in the signal-to-noise ratio (SNR) near 20 atmospheres as was expected from the arguments above.

IV.A. HIGHLY NONLINEAR ACOUSTIC RESONANCE

At high pressures and high acoustic intensities, we expect the sound
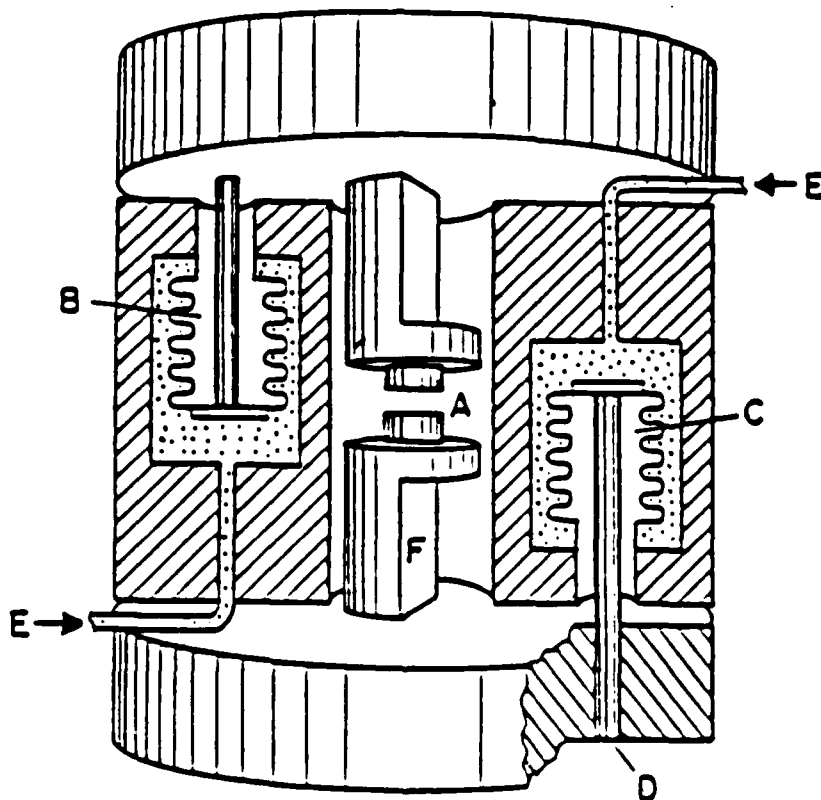
FIG. 11. Cutaway figure of the pressure cell. A. Sapphire rods
for the lens and the flat reflector. B and C. Miniature
bellows. D. Pushrod. E. Control capillaries.
F. Impedance matching circuitry.
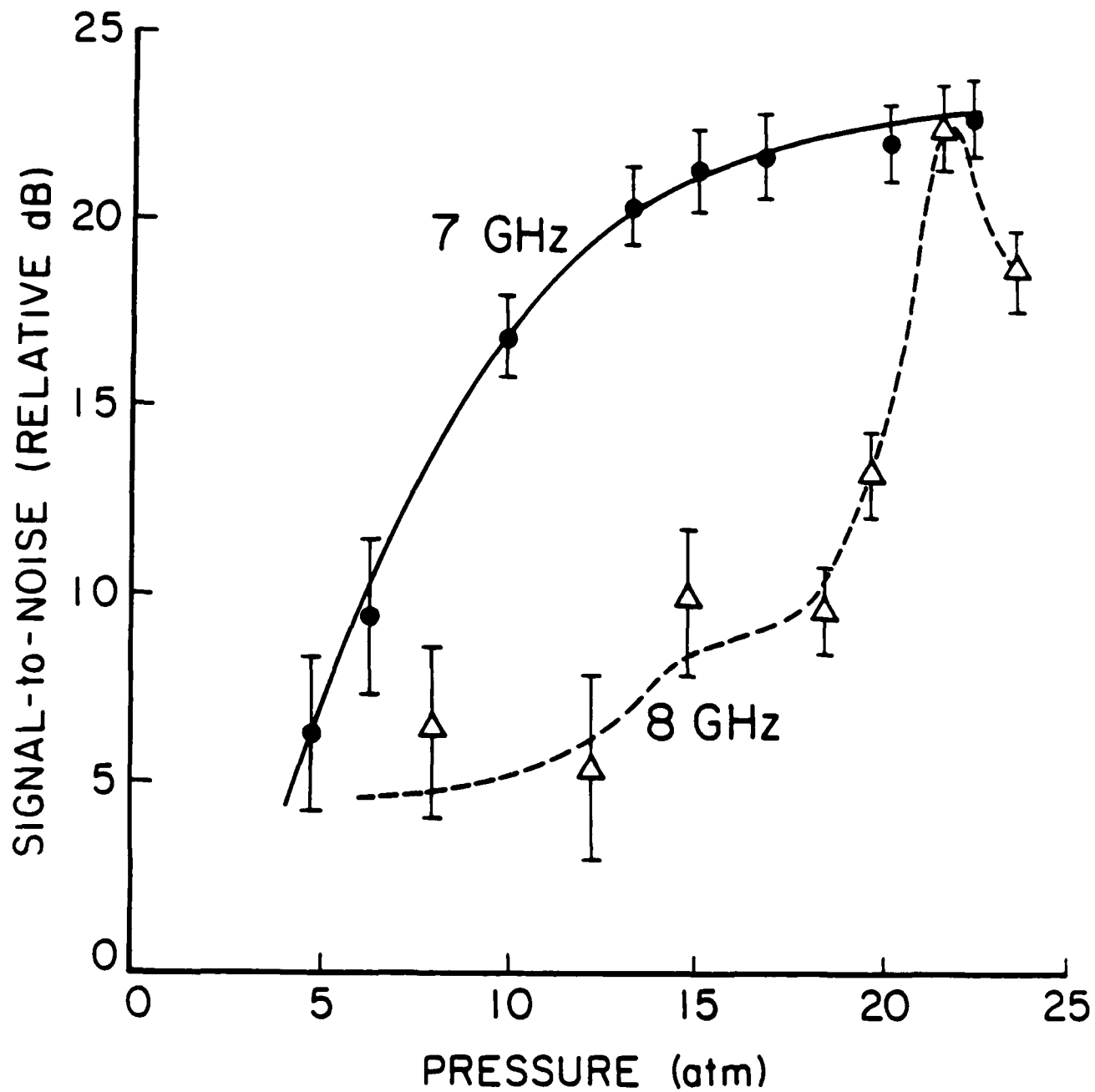
FIG. 12-- Improvement of SNR upon pressurization of helium at frequencies
of 7 and 8 GHz.

waves to generate many harmonics and form a converging shock wave. At this point, the sound intensity of the fundamental beam (which we measure) should saturate at a maximum value. This effect has been seen by many observers previously. However, in our experiments -using very high frequency coherent sound waves in pressurized superfluid helium - we see a very different kind of behavior. The intensity of the reflected pulse of a sound beam can actually decrease as the input power is increased. We have seen this previously with plane waves.[3] We have performed two experiments at 7 and 8 GHz with two different acoustic lenses to determine the behavior of high intensity sound wave propagation in case of focused sound beams.

Figure 13 shows the received power from an acoustic lens at 7 GHz focused on a flat sapphire sample. As the lens-to-sample spacing is varied, the received power changes. At the peak power, the lens is said to be in focus. At low pressures, the qualitative shape of the curve is the same independent of the input acoustic power (Fig. 13(a)). The shape is relatively unchanged as we go to pressures greater than 20 bar if we keep the input power low. But when the input power is turned up and the helium pressure is high, the shape of the focus changes dramatically (Fig. 13(b)). The curve shows some kind of resonant behavior where the received power oscillates with lens-to-sample spacing. Note that this behavior occurs when the sample is pulled away from the normal geometrical focus.

In the second experiment that we performed the frequency was 8 GHz and we used a different acoustic lens which was identical to the 7 GHz lens in terms of mechanical dimensions. The received power as a function of sample position is plotted in Figure 14 for low and high pressure and different input power levels. It can be seen that the behavior is different in this case at high pressure and high input powers. At low power levels

HIGH PRESSURE (19 atm)

RECEIVED POWER
(ARB. UNITS)

LOW POWER

HIGH POWER

(b)

z/λ

-2 0 2 4 6 8

LOW PRESSURE (13 atm)

RECEIVED POWER
(ARB. UNITS)

HIGH POWER

LOW POWER

(a)

-2 0 2 4

z/λ
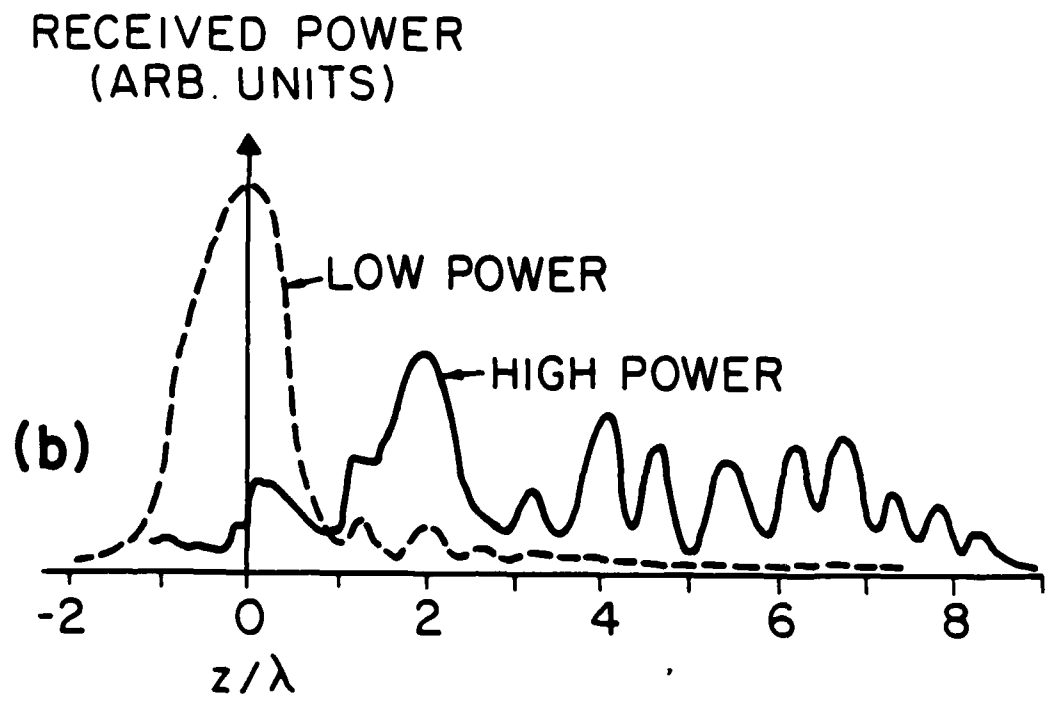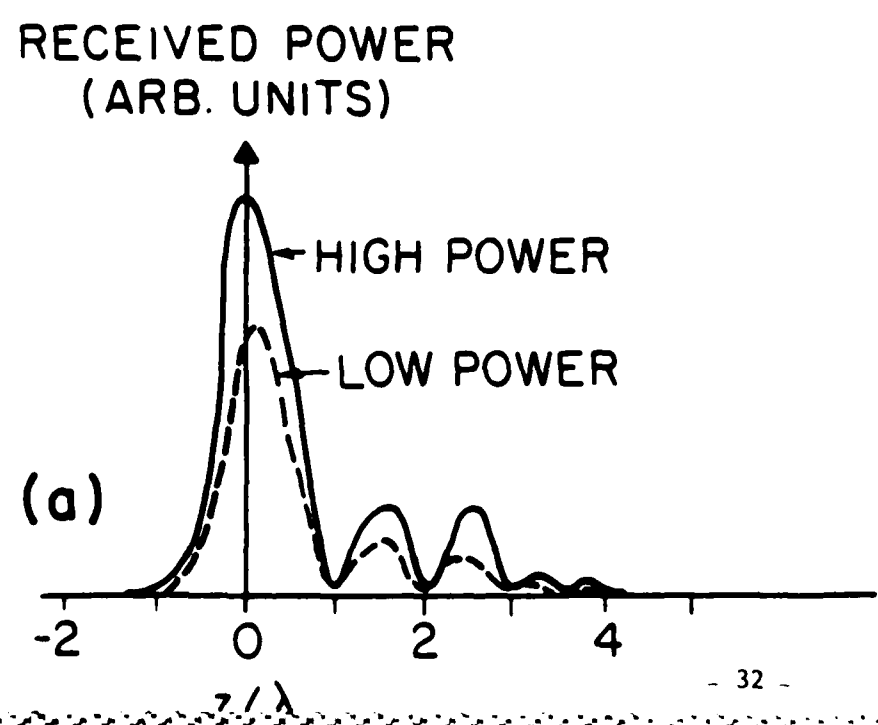
FIG. 13-- V(z) curves at 7 GHz. Positive z corresponds to moving away from lens. (a) At low pressures, increasing power has little effect on shape. (b) At high pressures and high powers, V(z) has extended structure several wavelengths beyond focus.

LOW PRESSURE (8 atm)

RECEIVED POWER
(ARB. UNITS)

LOW POWER

HIGH POWER

(a)

z/λ

-2   0   2   4   6

HIGH PRESSURE (24 atm)

RECEIVED POWER
(ARB. UNITS)

HIGH POWER

LOW
POWER

(b)

z/λ

-2   0   2   4   6
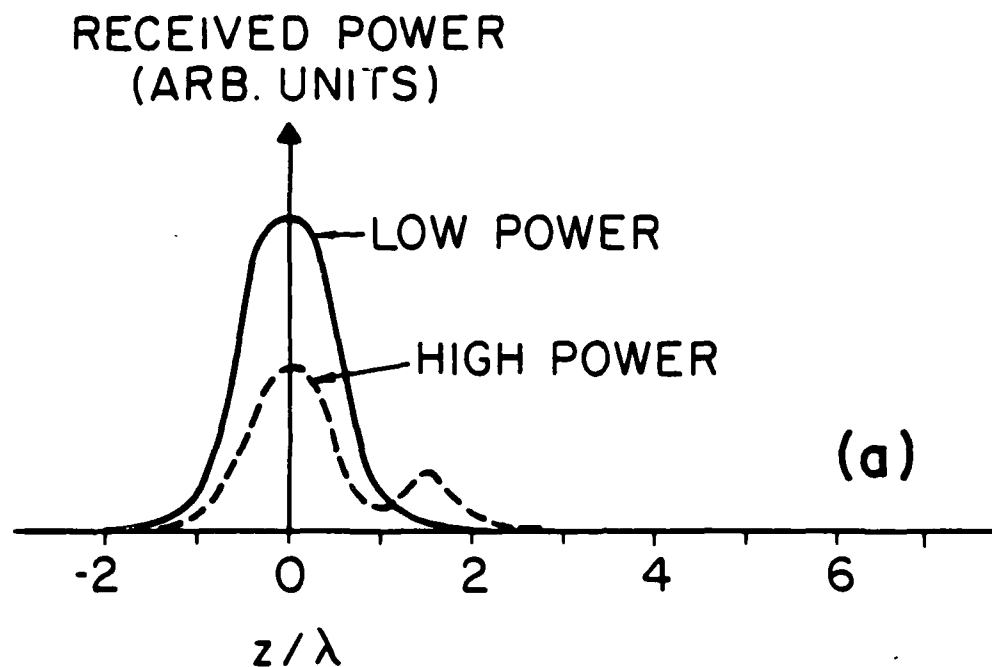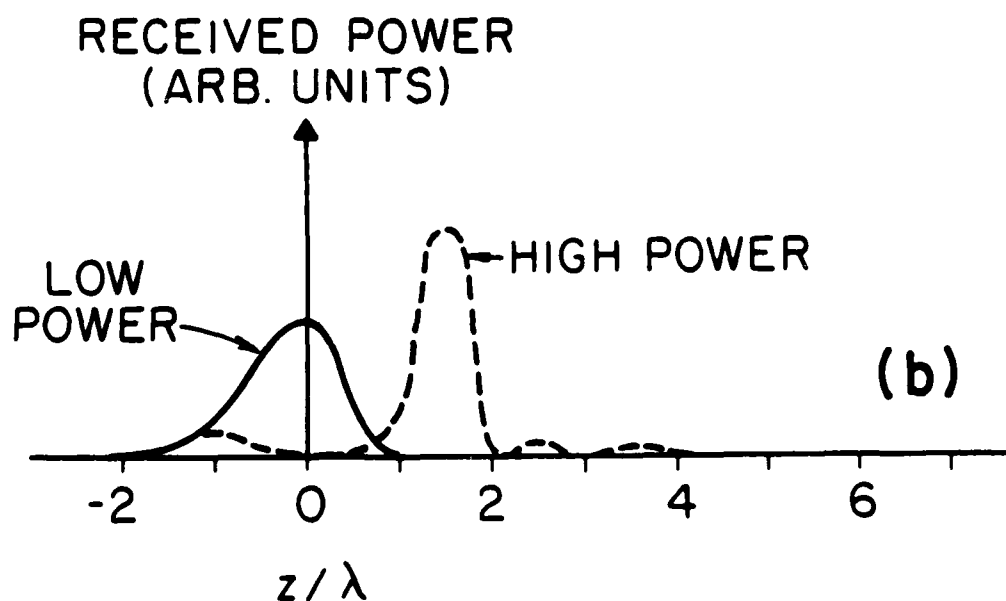
FIG. 14-- V(z) curves at 8 GHz. (a) At low pressures, increasing the input
power reduces the received power with little effect on the shape.
(b) At high pressures, increasing input power increases the received
power and shifts the main peak.

- 33 -

the received power is quite regular with one peak at the focus and nothing else at both positive and negative z positions at both low and high pressures. At high input power levels we see another peak appearing at positive z (sample away from the lens) at low pressures. At high pressure and high input power levels, we see the main peak shifting towards positive z positions and smaller peaks appearing as the sample is moved away from the lens. We do not find the oscillatory behavior observed at 7 GHz. We believe that the differences in the positioning of the transducer on the sapphire substrate which changes the illumination of the acoustic lens by the sound beam is responsible for the different behavior observed in the two experiments. Therefore, experiments as described above can be used to determine the quality of acoustic lenses. The lens used in the 7 GHz experiment is probably poorly illuminated by the sound waves coming from the transducer. The V(z) curve (received power vs. lens-sample spacing) contains more side lobes. At high input power levels the main lobe gets depleted because of parametric decay of sound and side lobes become much larger compared to the main focus.

IV.B. SOUND WAVE PROPAGATION AS A FUNCTION OF PRESSURE

We have also studied the nonlinear behavior of sound wave propagation quantitatively as a function of pressure in the 8 GHz experiment above. Plots of the output power as a function of the input power are shown for various pressures in Fig. 15, where the input powers are given in terms of the Mach number at the focus. The Mach number M is given by

$$M = (2I/\rho_0 c_0^3)^{1/2}$$

where I is the intensity of sound waves, ρ_0 and c_0 are the density and
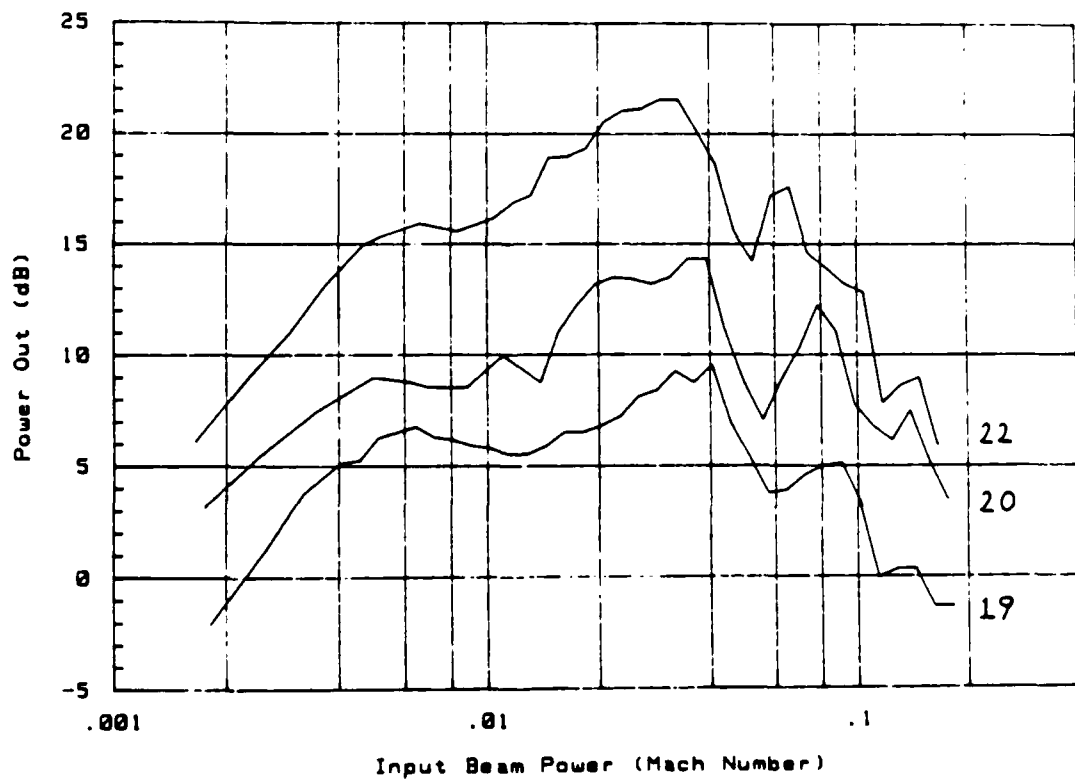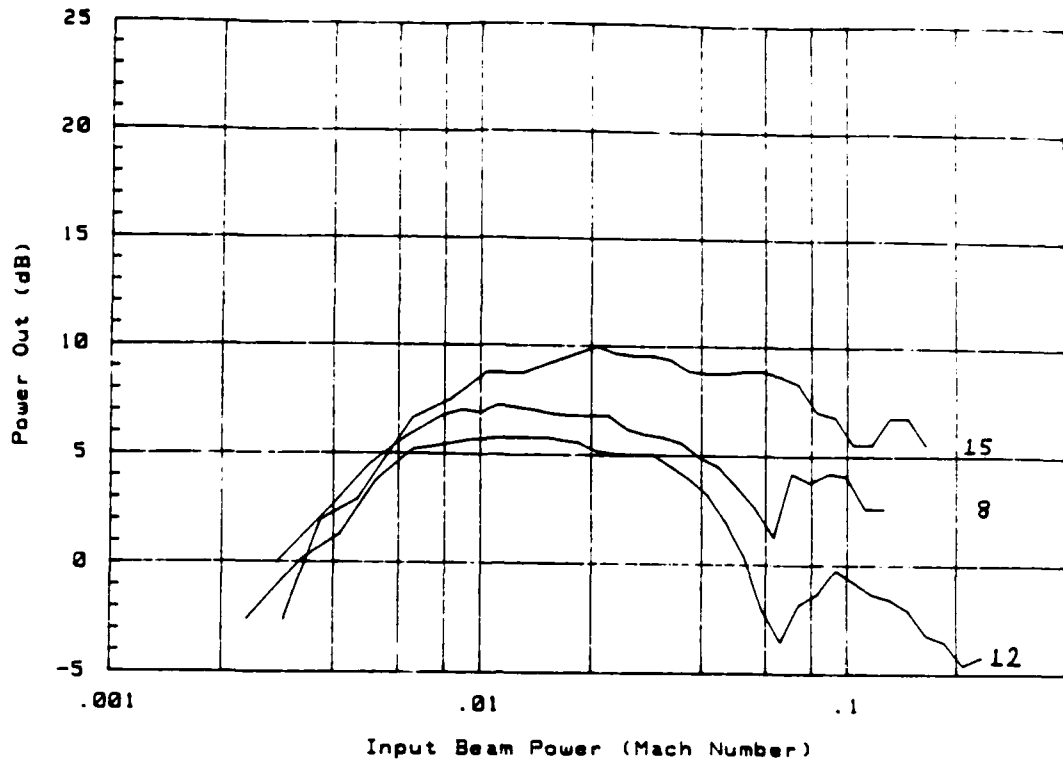
FIG. 15-- Power received (0 dB corresponds to noise of system) as function
of input intensity, given as Mach number at focus. Numbers next
to curves identify bath pressure in atmospheres.

speed of sound of the propagation medium, respectively. For each data point, the focus was adjusted until the signal was maximized. Three regions of pressure with different behaviors are observed. We will discuss each of these three regions in turn.

At low pressures, 8 bar and 12 bar, the dispersion curve is upward, or "anomalous," that is, the speed of sound increases with increasing frequency.[24] Spontaneous decay of the signal is thus possible using a three-phonon process (3pp) where the decay products have frequencies ω_1, ω_2, and wavenumbers k_1, k_2 satisfying

$$\omega_1 + \omega_2 = \omega_p; \quad k_1 + k_2 = k_p \qquad (1)$$

where the subscript p (=pump) refers to the input signal. The beam can thus spontaneously decay into two noncollinear phonons. Pump depletion is the result of parametric amplification of the stimulated decay products. Such behavior has already been reported for plane waves in superfluid helium.[3]

At an intermediate pressure, 15 bar, the dispersion is almost linear. As the dispersion gets more and more linear, the available angle between the decay products gets smaller and smaller. Hence we would expect sum processes to dominate. That is, the beam phonons are more likely to scatter off each other to produce harmonics than to scatter off the noise to decay. The beam power thus saturates (see Fig. 15) holding a constant power for a 15 dB range in input power.

At high pressures, 19 bar, 20 bar, 22 bar, the dispersion curve is now downward, so that neither the three-phonon decay of Eqn. 1 nor harmonic formation is phase-matched, that is, conserving both energy and momentum. As one adds increasing amounts of power to the system, however, the output, rather than saturating, continues to rise to a much

higher signal level. Then as more power is added, the output level actually *decreases*. The pump is then experiencing more than the simple saturation that might be expected in, say, shock wave formation, where additional energy is simply transferred into harmonics. A decrease in output with additional input would seem to be due to one of two causes. Either there is a major alteration in the nature of the medium, or there is a stimulated process occurring, in which phase-matched decay products are parametrically amplified at the expense of the pump. We will discuss each in turn.

A number of medium-altering effects associated with high-intensity sound propagation in liquid helium might account for the results at high pressure, namely cavitation, streaming, vorticity, and rapid melting and freezing. Above a certain critical amplitude, cavitation can result in massive signal loss. We did not, however, observe any of the usual increase in noise associated with cavitation and bubble collapse,[25,26] even using a spectrum analyzer. Also, evidence from another system indicates that the cavitation amplitude increases linearly with frequency, and extrapolation from helium experiments imply a much higher threshold than even the intensities used here.[27] On the other hand, the present amplitudes *are* larger than the onset for streaming reported in helium.[28] However, streaming is an effect most associated with continuous sound, and we were using short pulses and low duty cycles. The returned signal strengths were also independent of the pulse width and repetition rates. Furthermore, observations using a spectral analyzer showed no spectral (Doppler) shifts within the roughly 100 MHz bandwidth of the lens-amplifier system. Another possibile effect is that the intensity at the focus could be high enough to cause a small section of the superfluid to go "normal," due to the high vortex density. This process should be a

slow one[29] however, and experiments using multiple pulses showed that the pulses were completely independent/noninterfering on time scales as short as 100 nanoseconds. A final alternate explanation is rapid melting and freezing of the helium at the focus. This process is very fast, occurring at even gigahertz rates.[30] However, the output was very stable in time, and showed no abrupt change with increased bath pressure, as might be expected from a phase change, but rather showed a slow progression between the various regimes of pressure.

Having reasons to discount the helium-altering effects, then, we consider the possibility of a stimulated process. At high pressures the simple three-phonon process of Equation 1 cannot conserve both energy and momentum. The next simplest decay process which *can* conserve both is the four-phonon process in which two pump phonons scatter:

$$\omega_1 + \omega_2 = 2\omega_p; \quad k_1 + k_2 = 2k_p. \tag{2}$$

Referring back to Fig. 1, one also notices that the rate of drop of output signal with increasing input signal is twice as steep as that for low pressures. This result is consistent with Eqns. 1 and 2, since now *two* pump phonons are consumed in each stimulated decay event, versus one for the three-phonon process. Spontaneous decay (also called *parametric noise*) via four-photon processes has been observed in optics.[31,32] We believe these data to show the first observation of such a phenomenon in acoustics.

Our work shows that high frequency sound propagation in low-temperature helium is almost ideal for studying ultra-high nonlinearity, due to, for example, the absence of impurities, the lack of background noise (except quantum noise), and the high nonlinearity which can be manipulated by means of pressure. An intriguing possibility for a future experiment will be to increase the pressure above the freezing

point, repeating this experiment while propagating the sound in solid Helium-4. The possibility would then occur of observing transverse modes, which would follow a much different nonlinear equation.

IV.C. PARAMETRIC AMPLIFICATION

We have attempted, without success, to make an acoustic parametric amplifier in superfluid helium. The goal is two-fold : to increase the signal-to-noise ratio of the acoustic microscope by significantly decreasing the noise in the receiving system (by approximately 10 dB) and to further our understanding of resonant three-phonon processes in helium.

The key physical process in parametric amplification is stimulated decay. Figure 16 shows the process with a "pump" phonon colliding with the "signal" phonon. The signal phonon effectively stimulates the pump phonon to decay into two phonons, one which looks like the signal, and the "idler" phonon which is determined by conservation of energy and momentum. We see in this process that the signal has gain (it has doubled the number of phonons) and the pump has depleted. If the pump is very large, the signal will grow exponentially from parametric amplification.

The noise of the parametric amplifier is determined by the number of phonons in the superfluid helium which are similar to the signal phonons. Those include thermal phonons and zero-point phonons which can also be thought of as quantum noise. For our experiments, the temperatures are so low that the thermal noise can be disregarded and the quantum noise dominates. Therefore, an acoustic parametric amplifier in low temperature superfluid helium would have nearly lowest noise possible, more than a factor of 10 less than what we are presently using.

The experimental procedure of the amplifier is as shown in Figure 17. The pump and signal phonons are launched from a sapphire substrate into

PARAMETRIC AMPLIFICATION


STIMULATED
DECAY OF
PUMP
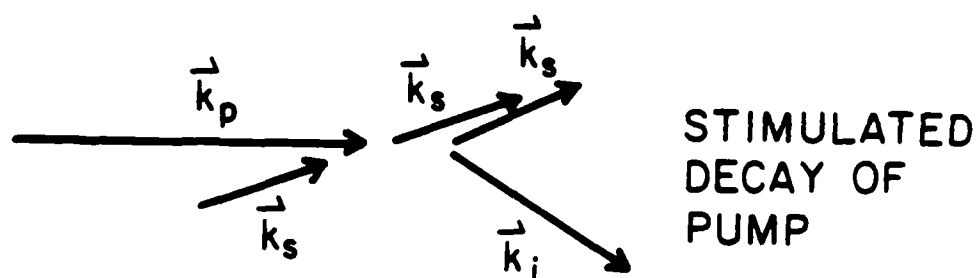
FIG. 16-- Diagram showing stimulated decay of pump phonon by interaction
with signal phonon, resulting in amplification of signal.

QUANTUM NOISE LIMITED
PARAMETRIC AMPLIFIER
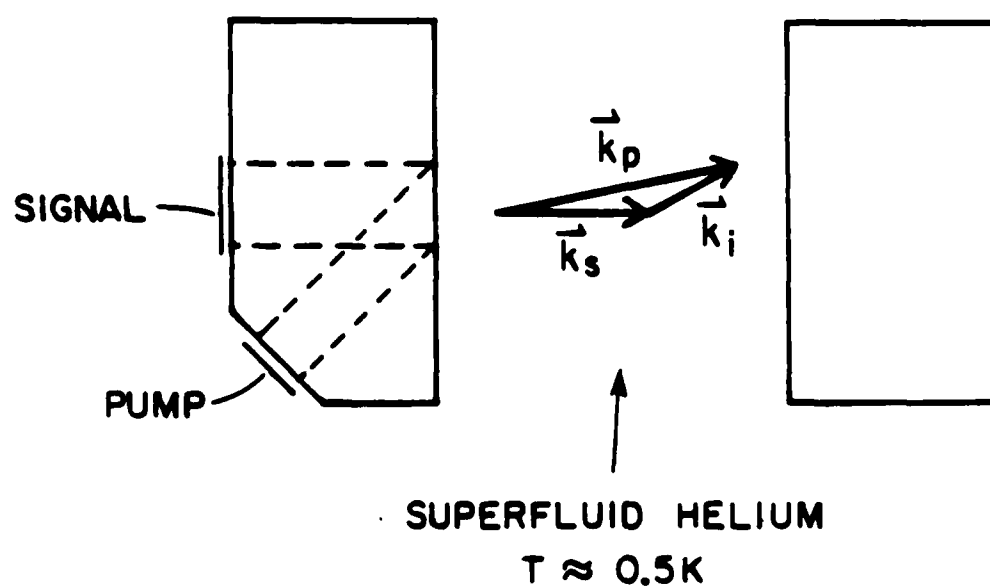
FIG. 17-- Experimental setup for parametric amplifier in helium.

liquid helium at an angle determined by the dispersion in helium and the frequencies of pump and signal waves. The signal phonons are amplified and detected by the same transducer after bouncing off a reflector surface. Unfortunately the short wavelengths that we are using impose severe requirements on the alignment of the two sapphire pieces and we have not been able to meet these requirements to see the signal reflected from the reflector piece.

V. MECHANICAL SCANNER

The mechanical scanner is one of the most important elements of the cryogenic acoustic microscope as its accuracy directly determines the quality of the image and the resolution of the microscope. The scanner unit of the old versions of the cryogenic acoustic microscope used a micrometer controlled rod extending to room temperature through the top-loader of the dilution refrigerator for focusing purposes.[1] We have seen previously that in order to obtain a reasonable signal-to-noise ratio of imaging at high gigahertz frequencies, the liquid helium cell has to be pressurized up to 20 atmospheres. The pressurization of the cell requires that this cell be sealed completely to withstand high pressures. Hence, the top-loading feature of the dilution refrigerator cannot be used to change samples nor to bring samples in and out of focus. So we had to design a new scanning unit to allow pressurization of the cell.

The requirements for the scanner can be summarized as follows. The fine X and Y scanning is used for taking images and the size of these scans should be at least 5 μm to get an adequate field of view. The fine Z scanner is used for fine focusing of the sample and should cover at least 5000 Å, several times the depth of focus of the microscope. The coarse Z focusing is needed because the samples are positioned such that they are millimeters away from the lens to avoid contact between the sample and the lens due to differential contraction of materials during cooldown. Coarse Z motion brings the samples near focus and must have a resolution of at least the range of the fine Z motion. The turnaround time of the refrigerator is approximately 4 days, 2 days for cooldown and 2 for warmup. Therefore, one would like to have some coarse X and Y scanning

- 4 3-

capability to image multiple samples during a single cooldown. These scanners must have a range of several millimeters to change samples with step sizes of tens of microns so as to look at adjacent areas on a sample.

All of the scanners mentioned above must be very rigid to avoid external vibrations to limit the resolution of the instrument. They must be small and compact to fit into the limited space of the refrigerator. The heat generated during scanning must be less than 100 µwatts to prevent temperature rise in the system. All these requirements make the problem of the design of the scanner a unique one.

The scanner previously used in the superfluid helium acoustic microscope also had problems with both accuracy and field of view. A moving coil - fixed magnet combination was used both to drive as well as to sense the motion. The system was not very rigid and room vibrations limited the accuracy to approximately 100 Å. The maximum field of view was 100 µm, limited by the ohmic heating in the superconducting scanning coils. Therefore, only a small area on a sample could be imaged in a single cooldown.

We have gone through three generations of scanner design during the period covered in this report. Figure 18 shows a diagram of the initial design. The fine scanning in X and Y directions are obtained using stacked piezoelectric ceramics which have sub-Å accuracy. To achieve a range of 5 µm a mechanical amplification scheme is required. A mechanical scanner with these specifications have been developed at the National Bureau of Standards by Scire and Teague.[33] Figure 19 shows a diagram of this scanner and the way it achieves mechanical amplification. We have built scanners using this design. The scanners we used in the initial design in Figure 18 had only a gain of 2.5. Since then we have built new fine scanners for the new versions of the scanning unit and obtained a
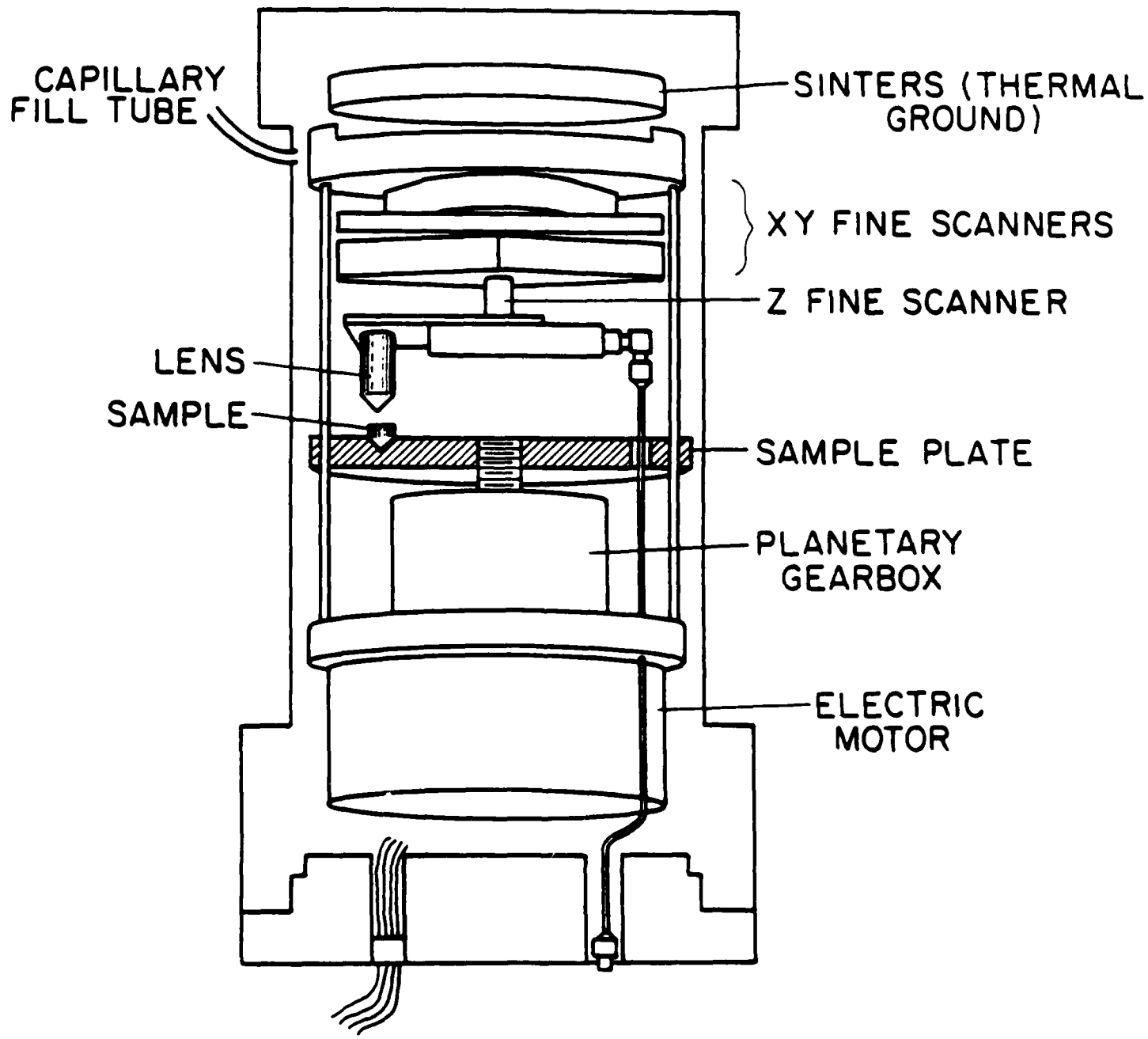
FIG. 18-- Diagram of scanner with motor controlled
coarse z-motion.
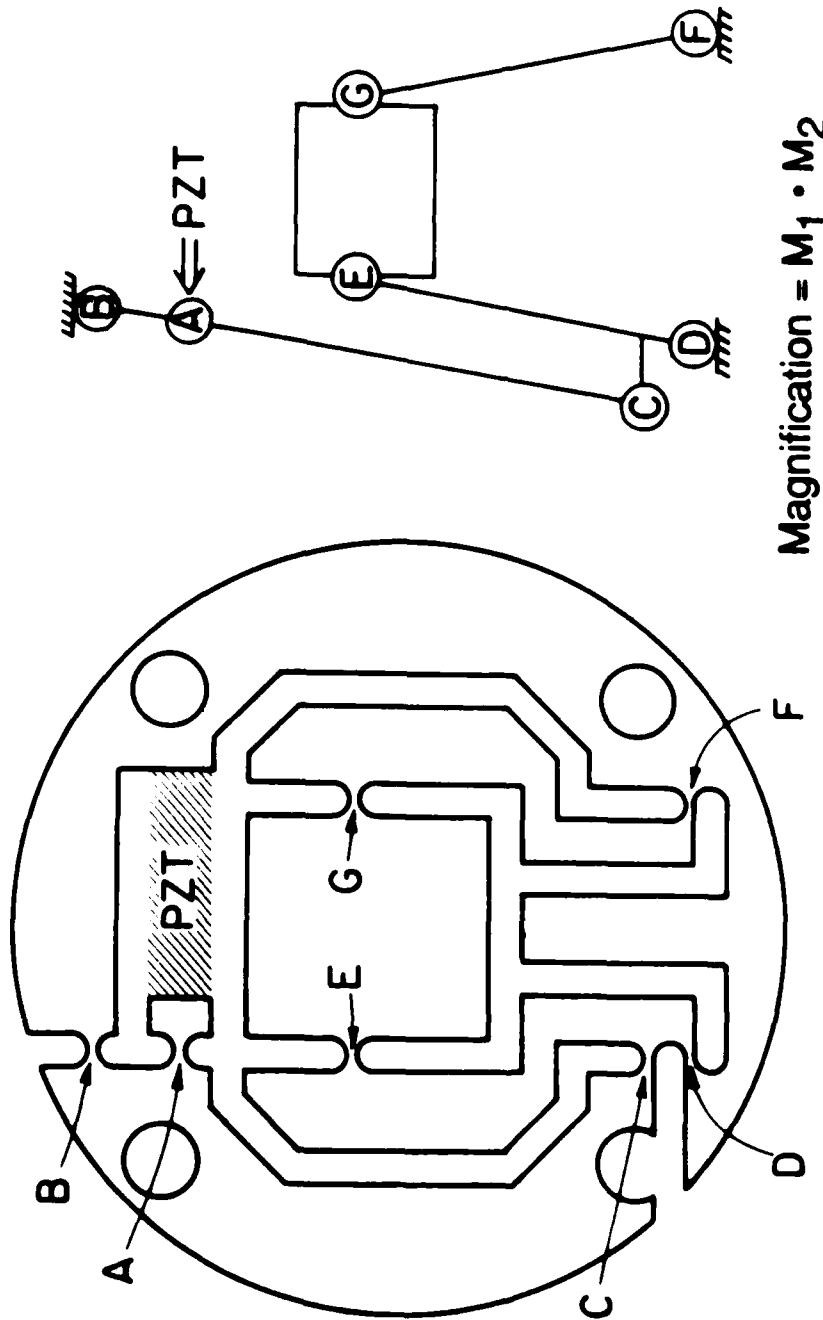
Magnification $= M_1 \cdot M_2$

$$M_1 = 1 + \frac{|A-C|}{|A-B|}$$

$$M_2 = 1 + \frac{|C-E|}{|C-D|}$$

FIG. 19-- Top-view of the fine scanner and principles of operation.

mechanical gain of nearly 5 at room temperature, providing a scanning range of 15 μm at liquid nitrogen temperatures. The Z fine scanner is simply a 0.5 inch long PZT tube which provides a motion of more than 5000 Å when cooled to liquid helium temperatures.

The scanner in Figure 18 did not have coarse X and Y motion capability as the main purpose was to test the coarse Z positioning. The original idea for the motion in Z direction was to use an electric motor. Since the final step size needed is extremely small, only 5000 Å, a gearing assembly is required to reduce the movement of the motor and to increase the torque supplied by the motor. The advantage of such a system is the ease of control and repeatability of steps. But the gears used in the system had to be degreased to enable operation in the low temperature and vacuum environment of the microscope. Even after the application of a common low-temperature lubricant, MoS, the friction in the gearbox remained relatively high, causing heavy loading for the motor. We tried several dc stepping motors and ac motors rewound with superconducting wires to reduce the heat dissipation due to ohmic heating of the coils. But all of these motors failed to operate reliably at cryogenic temperatures. The heat load in the refrigerator was still too large due to eddy current losses in the system.

After the failure of our attempts of using motor-gear assembly to provide Z motion for the microscope, we turned to another idea that was employed in the refrigerator a few years ago in an experiment to measure dispersion of sound waves in superfluid helium.[2] In this experiment coarse motion of a few millimeters was achieved by pneumatic bellows, pressurized by liquid helium administered by way of small capillary lines which exit the refrigerator to a gas handling system at room temperature. Motion is experienced by a steel rod attached to the moving end of a very

stiff stainless steel bellows as a pressure differential between the inside and outside of the bellows is applied. The heat load of this system to the refrigerator is usually very low, the only load being due to the liquid helium entering or exiting the bellows when pressure is changed. This system also has the advantage of providing smooth, continuous motion of up to a few millimeters which can be controlled to less than 1000 Å. The main drawback we had experienced with the older apparatus was a drift caused by pressure differences due to bubbling and height changes of the liquid helium in the capillary line which goes out to the gas handling system. The solution we proposed was an additional bellows, mounted perpendicular to the first, which would be used as a "lock," squeezing on the focusing rod so it would not slip.

Figure 20 shows the second generation scanner unit we built with bellows controlled Z motion. The fine X, Y and Z motion assemblies are identical to the first design. On the bottom of the cell a steel block containing the focusing and locking bellows replaces the motor gear assembly of the first scanner.

We tried the new scanner with an acoustic lens operating at a center frequency of 7 GHz. The wavelength of imaging was less than 500 Å at pressures near 20 atmospheres. We observed a few problems with the scanner during this experiment. The main problem was the limited range in the Z motion and locking system. This is because the system is assembled with no pressure applied to bellows. When pressure is applied to focusing bellows, it moves the sample towards the lens. To apply the lock with the locking bellows, inside pressure of the bellows also needs to be increased. But the microscope is normally operated with a pressure of 20 atmospheres in the cell to get a good signal-to-noise ratio of imaging and liquid helium freezes at pressures greater than 25 atmospheres at
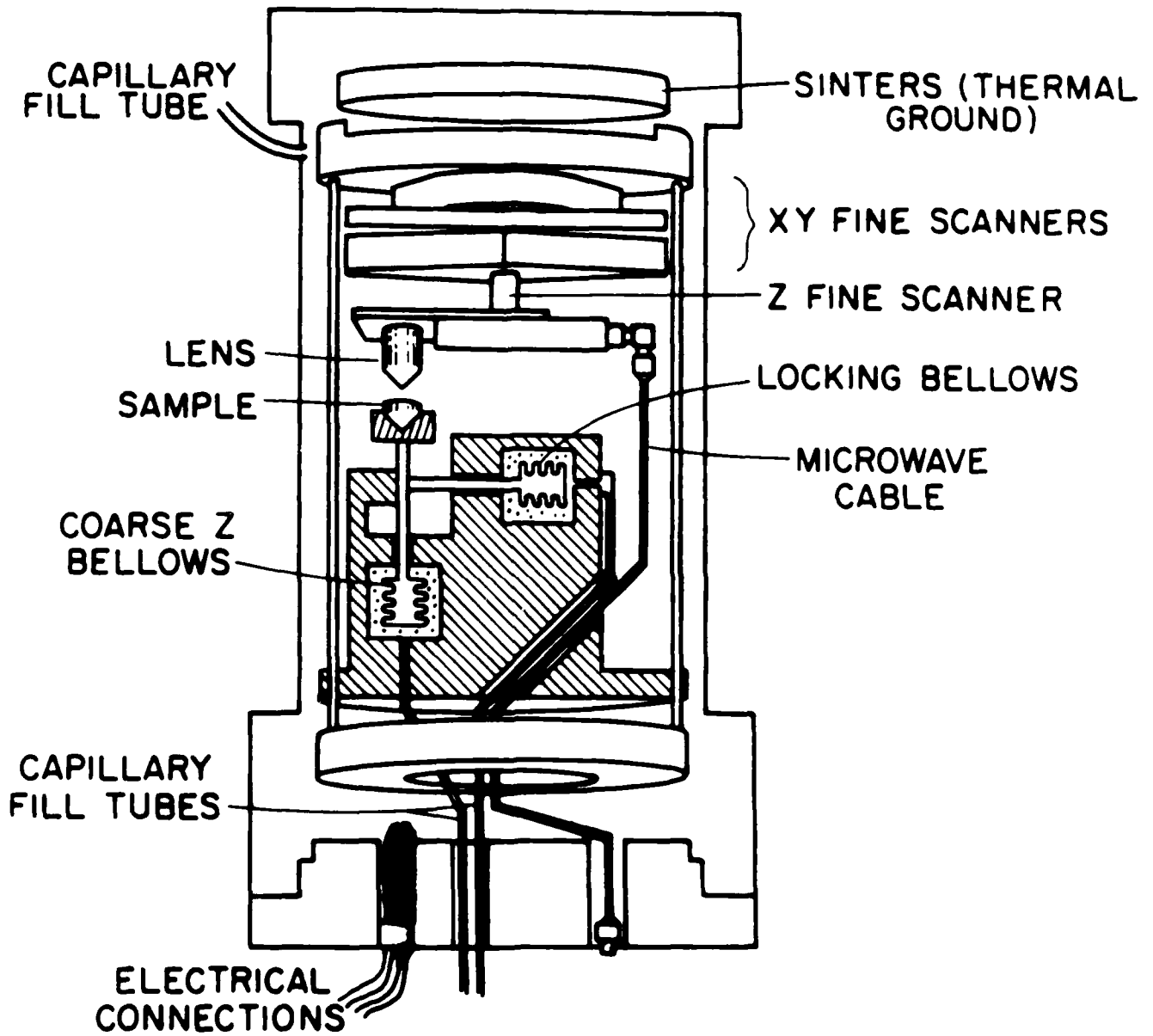
FIG. 20-- Diagram of the initial design of scanner with bellows
controlled coarse z-motion.

temperatures below 1 K. Therefore this system utilizes a pressure differential of only 5 atmospheres to move the bellows which is 1/5 of the maximum range that can be achieved. So the amount of locking was limited and we still observed some drift in the focusing. The system also required that the samples positioned to within much less than 0.5 mm of the lens at room temperature. This also created the possibility of accidental contact between the sample and the lens during cooldown when differential contraction might occur.

We then started working on the third version of the scanner. A diagram of the scanner is shown in Figure 21. The fine X, Y and Z scanners are still positioned at the top of the cell moving the lens assembly. The coarse Z scanner was modified as shown to solve the problems observed in the previous design. Both the focusing and locking bellows are turned around 180°. The focusing is controlled by two bellows (only one is shown in Figure 21), connected together by steel rods in the shape of a "W." The sample plate rests on the center pillar, and the bellows, when pressurized, push down on the sides of the "W," thus lowering the sample plate, i.e., increasing its distance from the lens. Therefore, the samples can be positioned near the lens with no pressure applied to the bellows and the bellows are pressurized to increase the separation between the lens and sample to avoid contact during cooldown. When imaging near a pressure of 20 atmospheres, the pressure in the bellows can be lowered to bring the sample in focus. The locking bellows are also turned around so that lowering the pressure brings the bellows to locking condition. Therefore this arrangement of bellows has nearly full use of the 25 atmosphere range possible in liquid helium.

The scanner in Figure 21 also has the capability of coarse scanning in X and Y directions. These scans are achieved by a simple coil-magnet

CAPILLARY FILL TUBE

SINTERS (THERMAL GROUND)

X Y FINE SCANNERS

Z FINE SCANNER

LENS

MICROWAVE CABLE

SAMPLE

X Y COARSE SCANNERS

LOCKING BELLOWS

COARSE Z BELLOWS

ELECTRICAL CONNECTIONS

CAPILLARY FILL TUBES
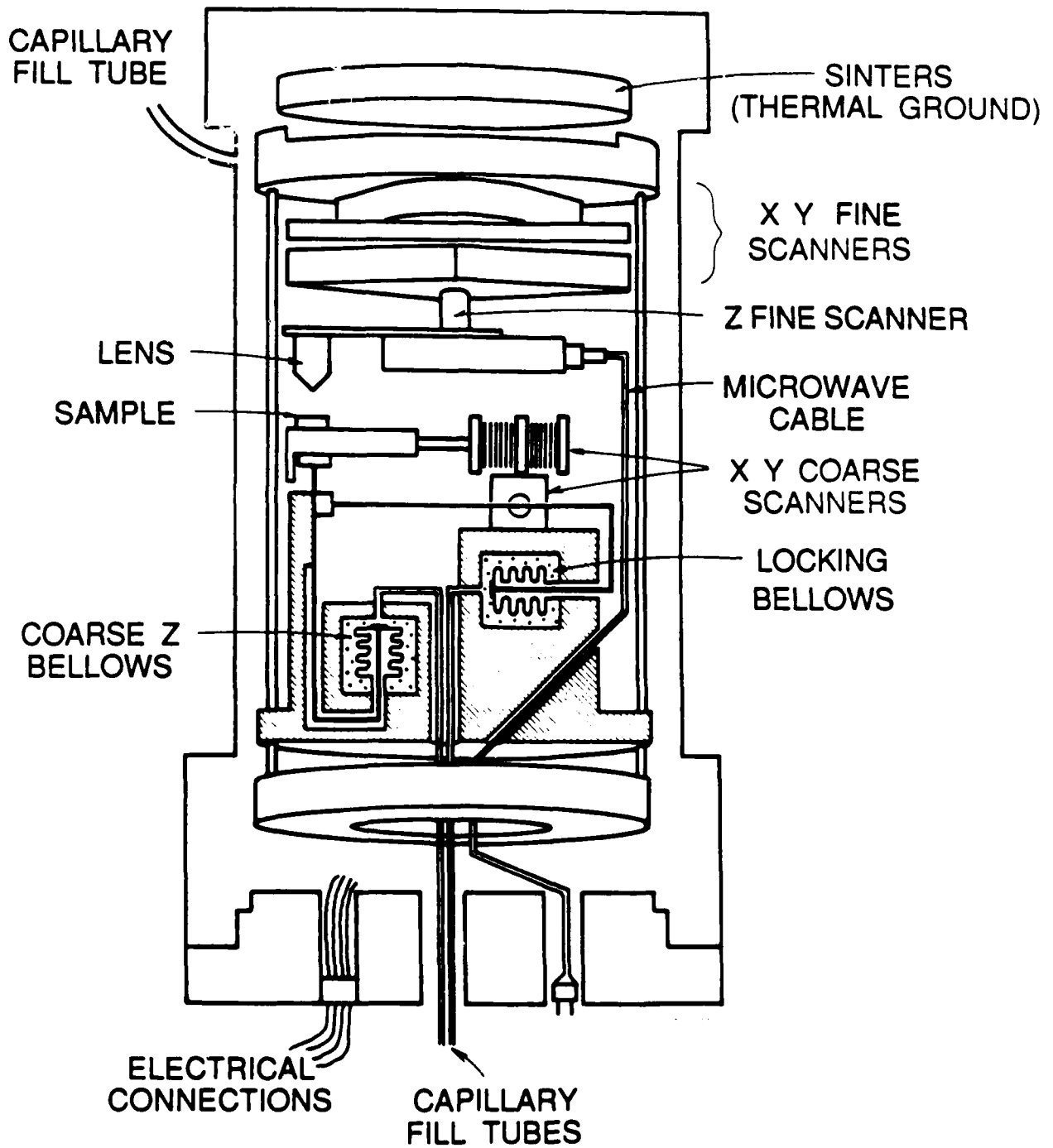
FIG. 21-- Cross-sectional view of the complete scanner assembly.

configuration. The system consists of two coils next to each other and a cylindrical magnet in the center of the coils. When a current pulse is applied to the coils, Lorentzian forces move the magnet in a direction depending on the polarity of the current pulse. The size of the steps are controlled by the friction in the system and the inertia of the magnets as well as the magnitude and duration of the current pulse. Two of these systems are orthogonally mounted on top of the coarse Z block and they move the sample plate in X and Y directions.

We have tested this scanner system with a 7 GHz acoustic lens and we were able to observe the acoustic reflections from the sample. The locking mechanism seemed to operate successfully. The drift in the focus appeared to be very small, less than 5000 Å in a time span of 30 minutes. The coarse X and Y scanners also operated successfully, taking steps on the order of tens of microns with a total range of nearly 5 mm. So it appears that the scanner is nearly ready for imaging samples with high resolution.

VI. CONCLUSION

With the development of high efficiency transducers operating at millimeter-wave frequencies and the new mechanical scanner, we are now in the process of setting up the microscope for operation at 32 GHz in superfluid helium. The acoustic wavelength in helium at this frequency is approximately 100 Å at a pressure of 20 atmospheres. So we should expect sub-100 Å resolution with this instrument.

We want to point out here that the millimeter-wave acoustic transducers we have developed can be useful in areas other than superfluid helium acoustic microscopy such as millimeter-wave technology. Millimeter-wave systems for communications, radar, plasma diagnostics, etc., are currently being developed by several industrial companies. High efficiency, low loss acoustic transducers can be used to develop signal processing devices such as resonators, delay lines and filters at millimeter-wave frequencies. We have discussed this program with some of the companies working on millimeter-wave devices and they have supported our research. Microwave Products Division of Hewlett-Packard helped us with the electronic instrumentation at 32 GHz. TRW has developed state-of-the-art HEMT transistors to be used in low-noise millimeter-wave receivers and they have agreed to help us with these receivers for experiments at a frequency of 32 GHz. The Aerospace Corporation also has a program on high frequency superfluid helium acoustic microscopy and they will especially benefit from the results of this research.

The high frequency acoustic transducers can also be useful to understand several physical phenomena such as sound attenuation at high

frequencies and phonon interactions in solids. Low frequency experiments[2,3,34] can be extended to millimeter-wave to understand the interesting dispersive - nonlinear properties of sound wave propagation in low temperature liquid helium.

LIST OF PUBLICATIONS

B. Hadimioglu, B.T. Khuri-Yakub, L.C. Goddard
and C.F. Quate
"Multi-layer ZnO Acoustic Transducers"
Proc. 1986 IEEE Ultrasonics Symposium, 1, 361 (1986)

B. Hadimioglu, L.J. La Comb, Jr., D.R. Wright,
B.T. Khuri-Yakub and C.F. Quate
"High Efficiency, Multiple Layer ZnO Acoustic
Transducers at Millimeter-Wave Frequencies"
Appl. Phys. Lett. 50, 1642 (1987)

D.R. Wright, B. Hadimioglu, L. La Comb, Jr.,
C.F. Quate and J.S. Foster
"Observation of the Pressure Dependence of
Nonlinear Interactions in a Focused Coherent
Acoustic Beam in Superfluid Helium"
To be published in Proc. 18th Intl. Conf.
Low Temperature Physics, 1987.

REFERENCES

1. B. Hadimioglu and J. S. Foster, "Advances in Superfluid Helium Acoustic Microscopy," J. Appl. Phys. **56**, 1976 (1984).

2. D. Rugar and J. S. Foster, "Accurate Measurement of Low-energy Phonon Dispersion in Liquid ^{4}He," Phys. Rev. B **30**, 2595 (1984).

3. J. S. Foster and S. Putterman, "Parametric Self Enhancement of Spontaneous Decay of Sound in Superfluid Helium," Phys. Rev. Lett. **54**, 1810 (1985).

4. F. S. Hickernell, "Zinc Oxide Films for Acoustoelectric Device Applications," IEEE Trans. Sonics Ultrasonics, **SU-32**, 634 (1985).

5. T. M. Reeder and D. K. Winslow, "Characteristics of Microwave Acoustic Transducers for Volume Wave Excitation," IEEE Trans. Microwave Theory and Techniques, **MTT-17**, 927 (1969).

6. B. Hadimioglu, "High Resolution Acoustic Microscopy," Ph.D. Dissertation, Stanford University (1985).

7. E. H. Jacobsen, "Experiments with Phonons at Microwave Frequencies," in *Quantum Electronics*, edited by C. H. Townes (Columbia Univ. Press, New York, 1960), p. 468.

8. J. B. Thaxter and P. E. Tannenwald, "Temperature Dependence of Attenuation of 70 Gc/sec Acoustic Waves in Quartz," Appl. Phys. Lett. **5**, 67 (1964).

9. J. Ilukor and E. H. Jacobsen, "Coherent Elastic Wave Propagation in Quartz at Ultramicrowave Frequencies," in *Physical Acoustics*, edited by W. P. Mason (Academic Press, New York,1968), **Vol. 5**, p. 221.

10. E. H. Jacobsen, "Sources of Sound in Piezoelectric Crystals," J. Acoust. Soc. Am. **32**, 949 (1960).

11. H. J. Shaw, "Selected Studies in Microwave Acoustics," Microwave Laboratory Report No. 1382, Stanford University (1965).

12. J. de Klerk, P. G. Klemens and E. F. Kelly, "Multilayer Enhancement of Microwave Piezoelectric Conversion in CdS-SiO Layers," Appl. Phys. Lett. **7**, 264 (1965).

13. E. K. Sittig, "Transmission Parameters of Thickness-Driven Piezoelectric Transducers Arranged in Multilayer Configuration," IEEE Trans. Sonics and Ultrasonics, vol. **SU-14**, 167 (1967).

14. K. H. Yang, P. L. Richards and Y. R. Shen, "Coherent Phonon Generation by Optical Mixing in a One-Dimensional Superlattice," J. Appl. Phys. **44**, 1417 (1973).

15. H. K. Wong, G. K. Wong and J. B. Ketterson, "Ferroelectricity and Coherent Phonon Generation in Piezoelectric Composition Modulated Structures," J. Appl. Phys. **53**, 6834 (1982).

16. P. Ruden and G. H. Döhler, "Anisotropy Effects and Optical Excitation of Acoustic Phonons in *n-i-p-i* Doping Superlattices," Solid State Communications **45**, 23 (1983).

17. J. J. Quinn, U. Strom and L. L. Chang, "Direct Electromagnetic Generation of High Frequency Acoustic Waves in Semiconductor Superlattices," Solid State Communications **45**, 111 (1983).

18. K. Dransfeld, "Quantum Aspects of Rayleigh Waves : Surface- and Interface Waves at Very High Frequencies," in *Rayleigh-Wave Theory and Applications*, edited by E. A. Ash and E. G. S. Paige (Springer-Verlag, Berlin, 1985), p. 110.

19. B. Hadimioglu. B. T. Khuri-Yakub, L. C. Goddard and C. F. Quate, "Multi-layer ZnO Acoustic Transducers," Proc. 1986 IEEE Ultrasonics Symposium, **Vol. 1**, 361 (1986).

20. J. S. Wang and K. M. Lakin, "Sputtered c-Axis Inclined ZnO Films for Shear Wave Resonators", Proc. IEEE 1982 Ultrasonics Symposium, 480 (1982).

21. R. C. Bray, "Acoustic and Photoacoustic Microscopy," Ph.D. Dissertation, Stanford University (1981).

22. V. B. Jipson, "Acoustic Microscopy at Optical Wavelengths," Ph.D. Dissertation, Stanford University (1979).

23. I. S. Ciccarello and K. Dransfeld, "Ultrasonic Absorption at Microwave Frequencies and at Low Temperatures in MgO and Al_2O_3," Phys. Rev. **134**, A1517 (1964).

24. H. J. Maris, "Phonon-phonon Interactions in Liquid Helium," Rev. Mod. Phys. **49**, 341 (1977).

25. R. Esche, "Untersuchung der Schwingungskaviation in Flüssigkeiten," (in German) Acustica **2AB**, 208 (1972).

26. E. A. Neppiras, "Subharmonic and Other Low-frequency Emission from Bubbles in Sound-irradiated Liquids," J. Acoust. Soc. Am. **46**, 587 (1969).

27. R. D. Finch, R. Kagiwada, M. Barmatz, and I. Rudnick, "Cavitation in Liquid Helium," Phys. Rev. **134**, A1425 (1964).

28. R. F. Carey, J. A. Rooney, and C. W. Smith, "Subharmonic Responses in Liquid Helium," J. Acoust. Soc. Am. **66,** 1801 (1979).

29. F. P. Milliken, K. W. Schwartz, and C. W. Smith, "Free Decay of Superfluid Turbulence," Phys. Rev. Lett. **48**, 1204 (1982).

30. T. E. Huber and H. J. Maris, "Capillary Effects on the Phonon Transmission between Liquid and Solid Helium," Phys. Rev. Lett. **47**, 1907 (1981).

31. D. L. Weinberg, "Four-photon Optical Parametric Noise in Water," Appl. Phys. Lett. **14**, 32, (1969).

32. J. G. Meadors, W. T. Kavage, and E. K. Damon, "Observation of Tunable Four-photon Parametric Noise in Calcite," Appl. Phys. Lett. **14**, 360 (1969).

33. F. E. Scire, E. C. Teague, "Piezodriven 50-μm Range Stage with Subnanometer Resolution," Rev. Sci. Instrum. **49**, 1735 (1978).

34. D. R. Wright, B. Hadimioglu, L. J. La Comb, Jr., C. F. Quate and J. S. Foster, "Observation of the Pressure Dependence of Nonlinear Interactions in a Focused Coherent Acoustic Beam in Superfluid Helium," to be published in Proc. 18th Int. Conf. Low-Temperature Phys. (1987).

END

FEb.

1988

DTIC